Yang *et al. Energy Mater* 2023;3:300027
DOI: 10.20517/energymater.2022.91

Energy Materials

Review

Open Access

Check for updates

Recent progress and prospect of Li-Se batteries: a comprehensive review

Zixiang Yang[1,#], Yangdan Lu[1,#], Zhaoying Wang[2], Hao Dong[3], Jingwen Lin[1], Yang Wang[1], Ming Qiu[3], Zhizhen Ye[1], Jianguo Lu[1,*]

[1]State Key Laboratory of Silicon and Advanced Semiconductor Materials, School of Materials Science and Engineering, Zhejiang University, Hangzhou 310027, Zhejiang, China.
[2]Center for Multidimensional Carbon Materials, Institute for Basic Science (IBS), Ulsan 44919, Republic of Korea.
[3]Institute of Nanotechnology, College of Physical Science and Technology, Central China Normal University, Wuhan 430079, Hubei, China.
[#]Authors contributed equally.

[*]**Correspondence to:** Prof. Jianguo Lu, State Key Laboratory of Silicon and Advanced Semiconductor Materials, School of Materials Science and Engineering, Zhejiang University, Hangzhou 310027, Zhejiang, China. E-mail: lujianguo@zju.edu.cn

How to cite this article: Yang Z, Lu Y, Wang Z, Dong H, Lin J, Wang Y, Qiu M, Ye Z, Lu J. Recent progress and prospect of Li-Se batteries: a comprehensive review. *Energy Mater* 2023;3:300027. https://dx.doi.org/10.20517/energymater.2022.91

Received: 14 Dec 2022 **First Decision:** 28 Feb 2023 **Revised:** 5 May 2023 **Accepted:** 26 May 2023 **Published:** 30 May 2023

Academic Editor: Yuping Wu **Copy Editor:** Yanbing Bai **Production Editor:** Yanbing Bai

Abstract

Developing high specific capacity electrode materials is definitely critical. Selenium (Se), with competitive electronic conductivity and high volumetric capacity, is regarded as one of the promising cathodes for next-generation lithium (Li) batteries. But the volume change and shuttle effect, together with loss of active material, result in poor lifetime and limited capacity. To alleviate these issues, various efforts have been made to optimize the performances of Li-Se batteries. This review summarizes the recent progress of the Li-Se system, especially the development of cathodes, with preparations, structures, electrochemical performances, and their relationships between structures and performances. The corresponding components are mentioned as well. We expect that Li-Se batteries will have a bright perspective in the energy storage area.

Keywords: Li-Se battery, Se cathode, lithium storage, energy storage systems

INTRODUCTION

Energy is an important driving force for development. In the face of an energy crisis, energy storage systems

are urgently necessary to maximize energy utilization. Chemical batteries, processing chemical energy-electricity conversion with high efficiency, are considered as promising energy storage devices. Lithium (Li)-ion batteries (LIBs) are based on Li-ions moving between electrodes in the electrolyte during (dis)charging while electrons flow through an external circuit. Li is the third lightest element and has one of the smallest ionic radii among singly charged ions[1]. This makes Li-ions have high mobility in the electrolyte and electrodes, facilitating their storage or release. Thus, the energy density of LIBs is very excellent (theoretical value of 387 Wh/kg), occupying a large share of the commercial battery market[2]. However, the capacity of the intercalated electrode is limited (the capacity of graphite anode is 372 mA h/g, and the capacity of $LiCoO_2$ cathode is 274 mA h/g), making the current LIBs unable to meet the increasing actual use needs[1,3,4].

As the cathode has low capacity, it is necessary to replace or renew its active materials. Compared with intercalation electrode materials, conversion electrode materials create and break chemical bonds during the insertion and extraction of Li-ions[5,6]. The conversion electrodes enable more Li-ions to participate in the reaction and migration and store more electrons. Thus, the capacity of insertion electrodes is lower than that of conversion electrodes. Among them, it may be appropriate for chalcogenide elements [sulfur (S), Selenium (Se), *etc.*] to match the Li anode. The lowest reduction potential of Li gives Li-based batteries a chance to have a high potential. As shown in Table 1, the Li-S battery has a high energy density of nearly 2,567 Wh/kg. However, the insulation performance of S and the shuttle effect of polysulfides lead to low coulombic efficiency and fast capacity decay. Se has a similar reaction that involves 2 electrons, corresponding to 1,155 Wh/kg. Due to the higher density of Se, the Li-Se battery can realize a volumetric specific capacity of 3,254 mA h/cm^3, which is equal to the Li-S battery (3,467 mA h/cm^3)[7-10].

In 2012, Abouimrane *et al.* first reported on the concept of Se cathodes and the fabrication of modern Li-Se batteries[11]. In recent years, it has been regarded as a potential practical candidate in the field of electrochemical energy storage. Jin *et al.* focus on micro/nanostructured electrodes for Li-Se batteries[12]. Gu *et al.* systematically introduced Se-based rechargeable metal batteries, which typically consist of a Se cathode and a metal anode (Li, Na, K, and Mg)[13].

Eftekhari *et al.* reviewed the main parts of the Li-Se system, which are the cathode, electrolytes, and separators[14]. However, they do not provide a full description of each of the components of the Li-Se battery, which are indispensable to form a complete energy storage device. In this work, the working mechanism and the latest research on Se cathodes for Li batteries are reviewed, together with their preparations, structures, electrochemical performances, and the relationship between structures and performances. In addition to Se, various Se-based cathodes are also studied. Spreading the electroactive materials throughout different matrixes is proven to improve the performance of the Li-Se battery effectively. Moreover, all the components of the Li-Se battery, cathode, anode, electrolyte, separator and interlayer, and even binder and current collector [as shown in Figure 1] are reviewed. Furthermore, the challenges and prospects for Li-Se batteries are also outlined.

PRINCIPLES AND CHARACTERISTICS OF LI-SE BATTERIES

Principles of Li-Se batteries

It is worth understanding the properties of Li, Se, and chemicals involved in the Li-Se system (e.g., conductivity, capacity, and solubility) for us, so we can better comprehend the characteristics and mechanism of Li-Se batteries. Li is a light metal with small mole mass of 6.9 g/moL and mass density of 0.53 g/cm^3. It can provide a quite negative electric potential and possess high theoretical specific capacity as an anode[15-17]. In addition, Li-ions with light weight and small ionic radii are suitable to be selected as charge

Table 1. Energy density and capacities of three Li-based batteries

Battery system	Li-ion	Li-S	Li-Se
Energy density (Wh/kg)	387	2,567	1,155
Specific capacity (mA h/g)	137	1,675	675
Volumetric capacity (mA h/cm^3)	700	3,467	3,254

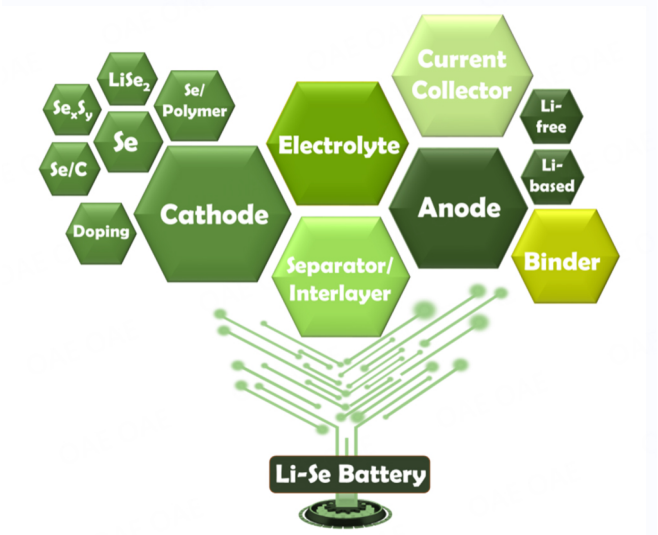

Figure 1. Composition of a Li-Se battery.

carriers. As for Se, trigonal Se (containing ordered Se_n chains) is thermodynamically stable and acts as a semiconductor at room temperature among several crystalline forms[12,18-21]. Compared with S (2.9 eV), Se shows a smaller band gap (1.7 eV), so it has much higher conductivity than that of S. The higher electronic conductivity makes Se-based cathodes become one of the competitive candidates for Li batteries. When coupled with a Li anode, the corresponding voltage of the Se cathode can reach 2.1 V[22,23]. The melting temperature of Se is 494.2 K, which is not very high for the preparation. In general, the Se cathode works normally over a wide temperature range (from ~298 K to ~423 K)[24-26].

Li-ions travel through electrolytes and react with Se in the cathode according to Equation (1).

$$Se + 2Li^+ + 2e^- \leftrightarrow Li_2Se \quad (1)$$

When Se transforms to Li_2Se upon Li insertion, it experiences a large volume expansion of about 98%. The phase transformation between trigonal Se and antifluorite Li_2Se is shown in Figure 2[11]. Fortunately, the final product Li_2Se owns high ionic conductivity and enables Li-ions to transfer rapidly into the cathode[27-29]. By studying the phase diagram of the Li-Se system, intermediates polyselenides produce when the Se cathode gets Li-ions from the electrolyte. Li polyselenides (Li_2Se_n, $n \geq 4$) are not thermodynamically stable, and their solubilities in various electrolytes are quite different[24].

There are two major types of organic electrolytes: ether- and carbonate-based electrolytes. Li, Se, and Li_2Se are slightly insoluble in both electrolytes. However, Li_2Se_n is dissolvable in DOL/DME (ether-based) electrolytes but insoluble in EC/EMC (carbonate-based) electrolytes [as shown in Figure 3][30]. Dissolved

Figure 2. Structural representations of trigonal Se and antifluorite Li_2Se[11]. Copyright 2012, American Chemical Society.

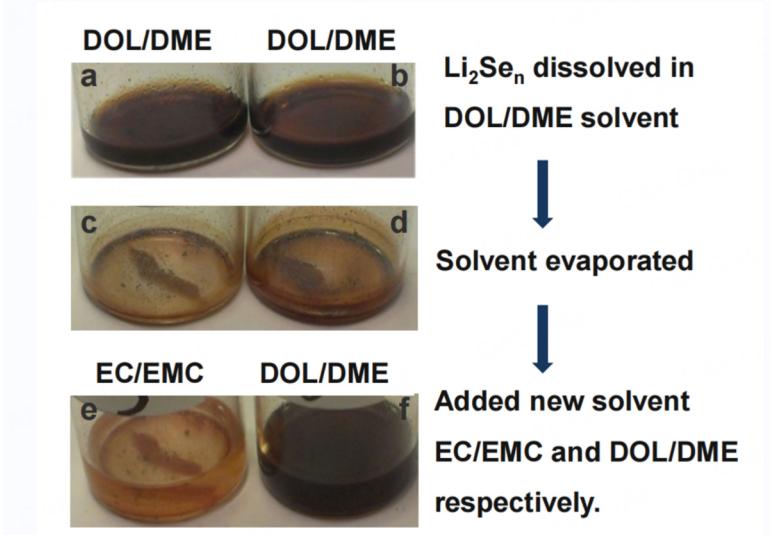

Figure 3. Li_2Se_n solubility testing of EC/EMC (carbonate-based) electrolytes and DOL/DME (ether-based) electrolytes[30]. Copyright 2014, The Royal Society of Chemistry.

polyselenides diffuse with the electrolyte and result in a side reaction with the anode, which causes the increase of electrolyte viscosity and fast decay of capacity seriously in ether-based electrolytes.

Mechanism and characteristics of Li-Se batteries

Amine *et al.* brought the concept of using Se as an electrochemically active material for Li batteries in 2012[11]. When discharging, the Li anode with a lower potential releases Li-ions and electrons to the cathode. Li-ions move toward the electrolyte to react with Se, while electrons flow via the external circuit to the cathode and output electricity. Se can receive up to two electrons per atom and experiences a series of changes in composition and structure to Li_2Se. When it is charging, the battery reverses the process under applied voltage. The overall redox reaction of Li-Se battery is

$$\text{Anode: } 2\,Li \leftrightarrow 2\,Li^+ + 2\,e^- \quad (2)$$

$$\text{Cathode: } Se + 2\,Li^+ + 2\,e^- \leftrightarrow Li_2Se \quad (3)$$

$$\text{Total: } Se + 2\,Li \leftrightarrow Li_2Se \quad (4)$$

However, the detailed reaction varies according to the solution of Li_2Se_n. The phase transition is single-step in carbonate-based electrolytes but multi-step in ether-based electrolytes, as Li_2Se_n is insoluble in carbonate-based electrolytes but soluble in ether-based electrolytes[29]. During the discharge in the ether-based electrolyte, Se is reduced to soluble Li_2Se_n first, then to insoluble Li_2Se_2 and Li_2Se. As shown in CV curves in

Figure 4A, there are two reduction peaks corresponding to the conversion of Se to Li_2Se_n, and then to Li_2Se_2 and Li_2Se, respectively. When charging, only one peak expresses direct oxidation of Li_2Se. In carbonate-based electrolytes, only one pair of reversible redox peaks is present in the CV in Figure 4C. It confirms the absence of Li_2Se_n and side reactions. In order to clarify the one-step mechanism, Cui *et al.* adopted bulk Se directly without carbon substrate and found that no polyselenides were observed in the carbonate-based electrolyte[30]. Other studies also demonstrated the direct transformation between Se and Li_2Se[31,32].

For Li-Se batteries in ether-based electrolytes,

Discharge:
Se to higher-order polyselenides:

$$Se + Li^+ \rightarrow Li_2Se_n\ (4 \leq n \leq 8) \quad (5)$$

higher-order polyselenides to lower-order polyselenides:

$$Li_2Se_n\ (4 \leq n \leq 8) + Li^+ \rightarrow Li_2Se_2 + Li_2Se \quad (6)$$

Charge:
Li_2Se to Se:

$$Li_2Se \rightarrow Se + Li^+ \quad (7)$$

For Li-Se batteries in carbonate-based electrolytes,

Discharge:
Se to Li_2Se:

$$Se + Li^+ \rightarrow Li_2Se \quad (8)$$

Charge:
Li_2Se to Se:

$$Li_2Se \rightarrow Se + Li^+ \quad (9)$$

Discharge/charge curves for the Se cathode in these two electrolytes are pictured in Figure 4B and D. Without the soluble intermediates in carbonate electrolytes, the suppression of shuttle effect and Se loss makes higher capacity and much better cycling stability.

Advantages of Se for Li-based batteries

As conversion electrode materials, chalcogens (S, Se, *etc.*) undergo two-electron reactions with Li. More electrons participate in the reaction and migration during the cycling[6], thus providing higher specific capacity and better rate performance. The competitive volumetric capacity of Se and the low solubility of polyselenides in some electrolytes enable the obstacles for Li storage to be overcome, as mentioned above. In carbonate-based electrolytes, it is generally believed that the solid Se is directly reduced to solid Li_2Se, which avoids the shuttle effect and the generation of intermediates. In addition, the conductivity of Se is

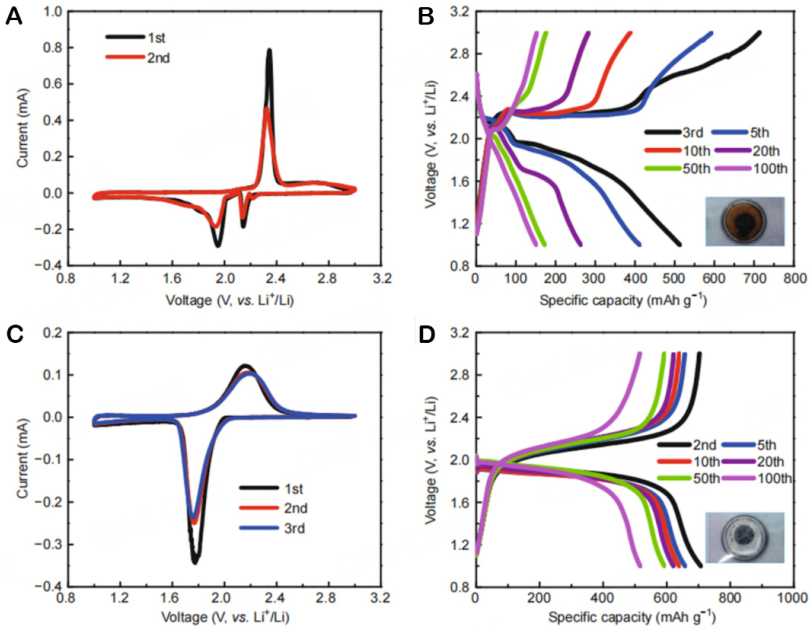

Figure 4. (A) CV and (B) discharge/charge curves for Se cathode with ether electrolyte. (C) CV and (D) discharge/charge curves for Se cathode with carbonate electrolyte[29]. Copyright 2015, Science China Materials. The insets of (B and D) show the disassembled cell after 100 cycles in ether- and carbonate-based electrolytes, respectively.

higher, which indicates that electrons migrate more easily through the cathode. Therefore, compared with insulating materials (such as S), Se has higher reactivity and better rate performance. In addition, the higher melting temperature reduces the chance of breakdown caused by battery overheating and ensures higher security for application.

In consequence, owing to the volumetric capacity together with the reaction kinetics and cycling stability, Se-based cathodes have great potential if they can make full use of the limited space, such as in the application of fixed energy storage (volume-constrained Li storage devices and large-scale batteries).

Issues with Li-Se batteries

Looking back on the lithiation/delithiation process, all the complex parts bring present risks for application. The widespread use of Li-Se batteries is hampered by several shortcomings.

Cost and safety. It is significant that the cost of Se is higher than that of S, the crust content is less, and the toxicity is stronger, which impedes its commercialization[1,33]. The toxicity of Se and some selenides may make people question the safety of Se for daily use[11,34-36]. Thus, Se is supposed to be sealed and treated properly in order not to hurt human health or the environment. Its large-scale applications will be greatly hindered by the limitation of all the cost.

Selenium loading rate. Due to the high expansion rate of Se itself, it is usually necessary to load it onto supports such as graphene. The load capacity seriously affects the capacity of the positive electrode material. Further research is needed on how to increase the Se load without affecting the stability of the normal operation of batteries[37].

Volume expansion. Since the crystal structure of the conversion electrode changes during cycling, the volume change is much more serious than that of the intercalation electrode. The space of Se crystals is

narrow enough to accommodate the insertion of Li atoms, and thus the volume expansion after discharge causes mechanical stress between the particles and structural damage to the cathode. During the long-term cycles, the loss of Se active materials results in fast capacity fading, short lifetime, and even pulverization of electrodes.

Slow reaction kinetics. Even if trigonal Se, which has the highest conductivity of all Se forms, is used as the cathode material, its middling conductivity is still at the level of the semiconductor. The slow rates and short distance of Li-ions diffusion and electrons in solid Se undermine the kinetics of reaction, resulting in poor utilization of Se and rate performance. The solid-solid transformation of Se to Li_2Se will be sluggish because of the slow diffusion kinetics of Li-ions and problems with charge transformation[38].

Shuttle effect of polyselenides. For the cathode, the transformation of Se to soluble polyselenides in ether-based electrolyte causes the loss of active material. In addition, the repeated diffusion and the reaction of polyselenides with electrodes lead to the deposition of insulators on the anode, the corrosion of solid electrolyte interphase (SEI) film, the consumption of electrolytes, and self-discharge of the battery. Coulombic efficiency and cycling stability are severely affected by existence of constantly moving polyselenides, which severely hinders the performance of Li-Se batteries. Thus, in addition to the certain toxicity and high cost, the electrical conductivity of Se is not high enough for fast electron transport. Besides, the serious volume expansion of Se and the shuttle effect of polyselenides result in low coulombic efficiency, low utilization rate of active materials, and fast capacity decay.

Improvement methods

According to research, Se nanoparticles (NPs) are promising for cancer treatment. Whether it harms human health depends mainly on the dose. Besides, the available electrolytes and electrode materials are also highly toxic. Therefore, the toxicity of Se should not hinder the development of Li-Se batteries.

It is not practical to use bulk Se electrodes. It is more feasible to find a porous matrix with enough space for the expansion and then spread the electroactive materials among it. Through spatial barriers and chemical binding, various conductive nanomaterials are used as a matrix to limit the volume expansion of electroactive materials. They have good electron conductivity and are necessary to solve the problem of low conductivity of the Se cathode.

Better electrochemical performance requires the combination of the advantages of electrodes and appropriate electrolytes. The proper electrolyte can greatly improve the utilization rate of Se and the battery cycle stability. This is due to high electron entry into the reaction center on the cathode, as well as the high Li migration rate of the cathode and the improved SEI layer on the Li anode. By forming a protecting layer on the electrode surface and suppressing the dissolution of intermediates, coulombic efficiency can be signally improved.

In addition, the use of suitable separators or interfaces is a practical method to block the polyselenides and restrains the side reaction. The shuttle effect can be overcome by a protective layer. Additives, binders (or even no binders), and current collectors are vital parts of reaching the overall performance (low cost, high capacity, and good stability), as many studies have found.

CATHODE MATERIALS OF LI-SE BATTERIES

Se

Se has a high specific capacity; however, it is of poor conductivity and evident expansion when reacting with Li. At present, technically pure Se cathodes are reported in the literature. However, problems may appear when it is used in practice.

Researchers have adopted some methods to optimize Se-based cathode since these properties tend to have significant impacts on the electrochemical performance of Li-Se batteries. Peng *et al.* encapsulated Se NPs in reduced graphene oxide (RGO) through a self-assembly process[39]. The introduction of NPs shortens the path of Li-ions, accelerates the diffusion of Li-ions, and improves the utilization rate of active materials. Thus, the Se@RGO cathode with a large Se content of 80 wt.% shows high capacity of 533 mA h/g at 0.2 C. When the current density increases by ten times from 0.5 to 5 C, the capacity retention reaches 73.3%, as shown in Figure 5A. Liu *et al.* prepared nanoporous Se (NP-Se) and commercial Se particles (CP-Se) cathodes and compared their electrochemical performances, respectively[40]. NP-Se is built up hierarchically with nanopores and nanowalls, avoiding aggregation and retaining small dimensions and large surface areas. As shown in Figure 5B, NP-Se cathode delivers initial capacity and reversible capacity after 20 cycles, higher than that of CP-Se cathode.

The thickness of Se nanowires sealed in the polyaniline (PANI) layer is about 25 nanometers, forming a core-shell structure [Figure 6]. The G@Se/PANI displays an accommodation of volume expansion, keeps the structure of active materials intact, and provides a short diffusion length for electronic/ionic transport[41]. Compared to bulk Se, Se nanowires cathode with one-dimensional structure exhibits better performance[42]. Through different polymer templates, nanostructured Se with controlled structures and sizes can be obtained easily. It can be used to construct Se particles in rod-like shapes, large spheres ($d > 1$ mm), small spheres ($d < 300$ nm), or hexagons, which helps the construction of cathode with high loadings and high areal capacity[43].

Se_xS_y

Se possesses competitive conductivity, but it is hindered by mass capacity and cost. S provides high capacity, but it has poor electrical activity. S atoms can be accommodated in the fully crystalline Se so that no S phase is formed[20,44-47]. In view of the above problems, the integration of Se and S into the binary compound cathode is expected to take advantage of their respective advantages while largely offsetting their disadvantages. It is natural to design Se_xS_y as an active material, as it has the ideal advantages inherited from elements S and Se, high capacity, feasible electronic conductivity, and moderate cost.

Abouimrane *et al.* demonstrated that Se_xS_y has higher capacity than Se alone[11]. The capacity increases as S content increases because of its contribution to total capacity. Cui *et al.* confirmed that Li/SeS_x battery has long cycle life and high efficiency in reversible cycle performance[28]. In the ether-based electrolyte, after 50 cycles, the discharge capacities of Li/Se, Li/SeS_2, and Li/SeS_7 systems are 350, 571, and 833 mAh/g, respectively [Figure 7]. A Se sulfide (SeS_x)/carbonized polyacrylonitrile (CPAN) composite material was synthesized by the vacuum annealing of a mixture of SeS_2 and polyacrylonitrile (PAN). $SeS_{0.7}$/CPAN maintains a reversible capacity of 780 mA h/g and exhibits slow capacity decay [Figure 8]. Later, confined by 70 wt.% of SeS_2 in a very ordered mesoporous carbon (CMK-3) framework with a protective sheath of polydopamine (PDA), the cathode achieved a capacity of more than 1,200 mAh/g at 0.2 A/g[48]. After coating with PDA, the surface looks much smoother than the bare particles [Figure 9A-C], and the escape of polysulfide/multi-selenide is inhibited [Figure 9D]. Under the protection of PDA, the CMK-3/SeS_2@PDA exhibits better cycling and rate performance [Figure 9E-G]. Se_nS_{8-n}/nitrogen (N)-doped mesoporous carbon

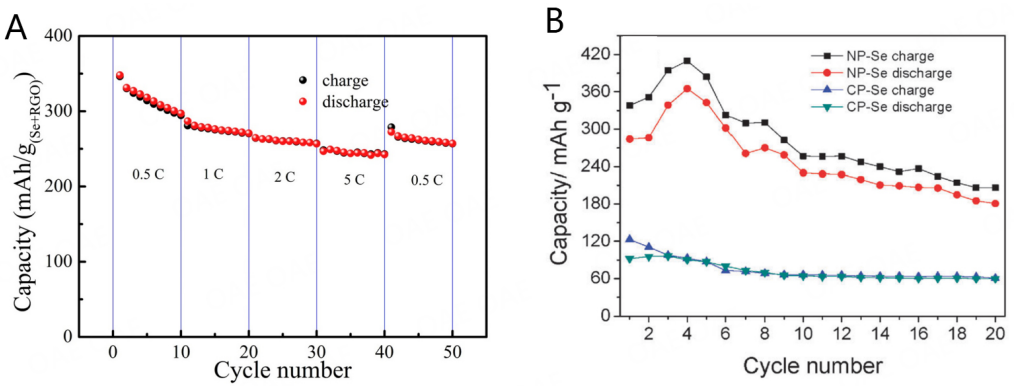

Figure 5. (A) Capacities at various C-rates ranging obtained from the Se@RGO composite cathode[39], Copyright 2015, Elsevier. (B) Cycling behaviors of NP-Se and CP-Se at a current density of 100 mA/g in the voltage range of 0.8-4.3 V[40]. Copyright 2013, The Royal Society of Chemistry.

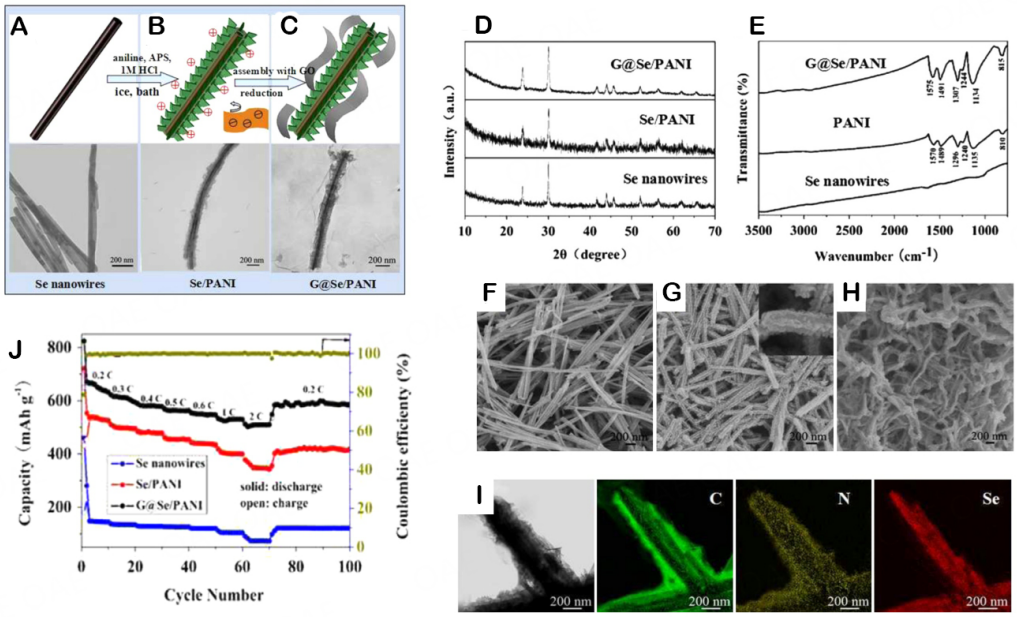

Figure 6. (A-C) Schematic illustration for the formation of G@Se/PANI, (D) XRD patterns and (E) FTIR spectra of the Se nanowires, Se/PANI and G@Se/PANI, (F) SEM and TEM images of Se nanowires, (G) Se/PANI and (H) G@Se/PANI, (I) elemental mapping images of G@Se/PANI (Carbon signal is green, Nitrogen signal is yellow and Se signal is red), (J) rate capability at various current densities between 1.0 and 3.0 V[41]. Copyright 2015, Elsevier.

(NMC) composites were prepared by uniformly limiting heteroatomic Se_nS_{8-n} molecules to NMCs. Figure 9H is a schematic diagram of the charging and discharging processes of S_8/NMC and Se_nS_{8-n}/NMC. After research, it was found that S_nS_{8-n} is uniformly captured in the mesoporous channels of the NMC matrix and forms strong interactions with N-doped carbon hosts [Figure 9I and J]. Se_2S_6/NMC showed excellent cycle stability and high rate efficiency [Figure 9K-M] 883 mA h/g after 100 cycles[49]. Se-S species bind with substrate more strongly than homoatomic S molecules, thus suppressing the shuttling phenomenon more efficiently. Thus, with higher specific capacity and economic benefit than Se and improved conductivity and stability compared to S, Se_xS_y cathodes continue to spring up and develop rapidly.

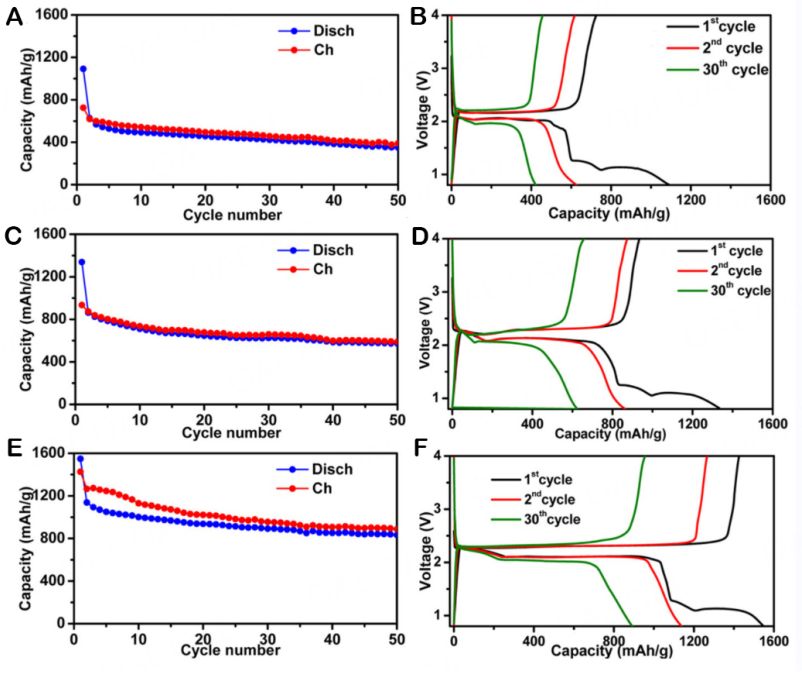

Figure 7. Cycle performance of Li cells with (A and B) Se-, (C and D) SeS_2-, and (E and F) SeS_7-carbon composite as cathodes in ether-based electrolyte[28]. Copyright 2013, American Chemical Society.

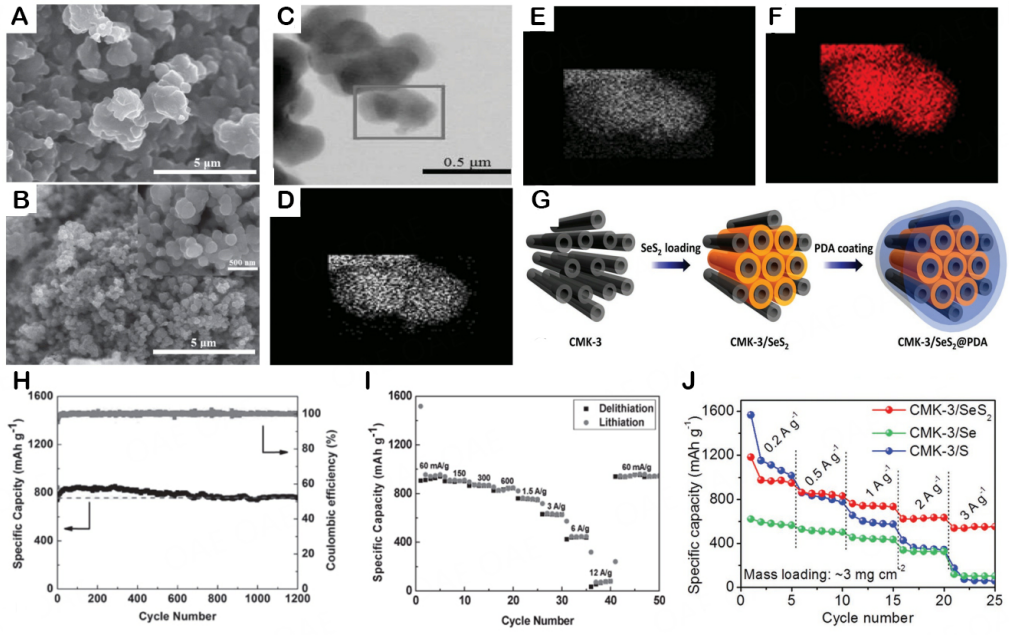

Figure 8. SEM images for PCPAN (A) and SeS_x /CPAN composites (B), TEM image of SeS_x/CPAN composites (C) and EDS elemental mapping images of the SeS_x/CPAN composites, marked by a square, for carbon (D), sulfur (E) and selenium (F), (H) delithiation capacity and coulombic efficiency versus cycle number at the current density of 600 mA g^{-1}, (I) rate performance at various C-rates[46], Copyright 2014, Wiley-VCH. (G)The synthetic process involves filling SeS_2 within nanochannels of CMK-3 to form CMK-3/ SeS_2, followed by coating PDA sheath to obtain the CMK-3/SeS_2@PDA composite, (J) Specific capacities of CMK-3/ SeS_2, CMK-3/Se, and CMK-3/S at various current densities[48]. Copyright 2017, Wiley-VCH.

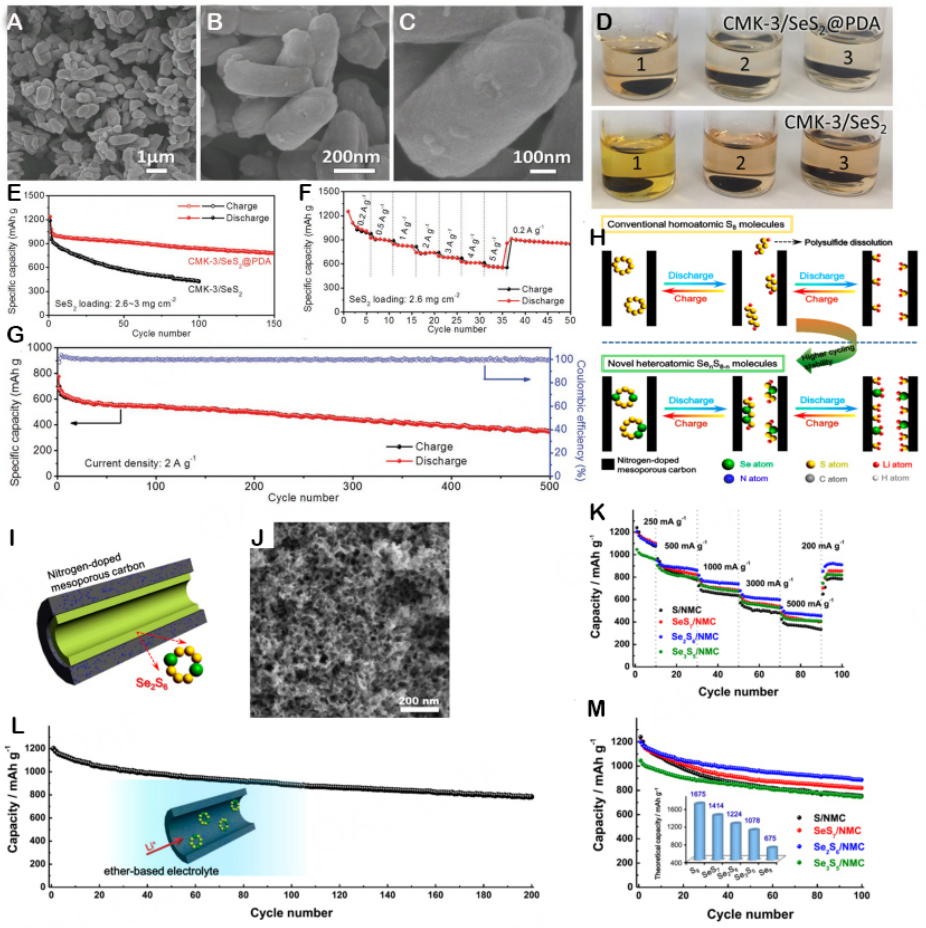

Figure 9. (A-C) SEM images of CMK-3/SeS_2@PDA, CMK-3/SeS_2@PDA, and (D) CMK-3/SeS_2 were disassembled, and their corresponding cathode electrode films were taken out and immersed in DOL solvent for 2 h, (E) Comparison of cycle performance between CMK-3/SeS_2 and CMK-3/SeS_2@PDA at a current density of 0.2 A g^{-1}, (F) Rate performance at various current densities from 0.2 to 5 A g^{-1} of CMK-3/SeS_2@PDA, (G) Prolonged cycle life of CMK-3/SeS_2@PDA at a current density of 2 A g^{-1} [48], Copyright 2017, Wiley-VCH. (H) Schematic diagram of the discharge-charge process of S_8/NMC and Se_nS_{8-n}/NMC, (I) Schematic model of the Se_2S_6/NMC structure, (J) SEM images of NMCs, (K) Rate performances of Se_nS_{8-n}/NMC (n = 1-3) at different current densities, (L) Long-term cycling performance of Se_2S_6/NMC at 250 mA g^{-1}, (M) Cycling performance of Se_nS_{8-n}/NMC (n = 1-3) at 250 mA g^{-1} [49]. Copyright 2016, American Chemical Society.

Li_2Se

The Li-S battery has received considerable attention earlier than the Li-Se battery. Thus, the former can be a good example to provide guidance for the development of the latter. Recently, given the new prospects opened up by Li_2S[50-52], research about Li_2Se has come into the field of Se-based cathodes gradually. The theoretical gravimetric and volumetric capacities of Li_2Se can reach 578 mA h/g and 1,659 mA h/cm^3, respectively. Li_2Se participates in the Li-Se reaction and is able to be paired with Li-free anode (such as C, Si, Sn, *etc.*), which obviates the formation of Li dendrite. It can be proved that Li_2Se has a lower Li-ion migration barrier than Li_2S by density functional theory calculation[27]. The conductivity and ion mobility of Li-ions in Li_2Se are higher than those of Li_2S, which makes Li_2Se even more promising. Moreover, there is no further volume expansion during the discharge, which avoids interactions between particles and enhances the mechanical strength of the electrode. However, the formation of Li_2Se and further process suffer from its high melting temperature (approximately 1,302 °C)[53-55].

Wu *et al.* synthesized Li_2Se cathode using Se powder and Li super hydride solution[53]. They found that the produced C-Li_2Se@C/Li cell shows high-rate capability and promising cycling stability. The cycling test demonstrates its discharge capacity of 300 mA h/g (C/2) after 100 cycles with no degradation virtually. No Li dendrites can be observed on cycled Li anode since polyselenide dissolution is reduced significantly. Moreover, C-Li_2Se cathodes show lower Li extraction overpotential and overcharging degree [Figure 10A and B] and smaller voltage hysteresis and better rate performance than Li_2S [Figure 10C and D], which is advantageous for applications.

Metal selenides

As cathode materials of Li-Se batteries, metal selenides are considered to improve the conductivity of electrodes, provide different electrochemical processes, or enhance the adsorption of soluble polyselenium intermediates through their polarity. In addition, its different nanostructures endow the cathode with different functions for Li-Se batteries and can promote redox kinetics. These metal selenides based on conversion reactions are also suitable for the anode of future Li-ion batteries[56-61].

Xue *et al.* prepared the $NiSe_2$ film cathode material by reactive pulsed laser deposition[62]. $NiSe_2$/Li cell achieves a large discharge capacity of 351.4 mA h/g as nearly all the inserted Li^+ can be reversibly extracted. Both Ni and Se provide the redox active centers in the reaction with Li. The high electronic conductivity of $NiSe_2$ improves the electrochemical reactions, leading to a high coulomb efficiency of close to 100%. Yang *et al.* prepared Co-porous carbon composites (Se@$CoSe_2$-PC) in one-pot reaction and then loaded Se via a melt-diffusion method[63]. As shown in Figure 11, in the copper (Cu)-doped $SnSe_2$ nanosheet composites, $SnSe_2$/0.4Cu samples show the best Li storage performance, exhibiting a reversible capacity of 583 mA h/g at a 0.1 C, and after 100 cycles, it still exhibits 254 mA h/g. The cathode based on Se@$CoSe_2$-PC offers an innovative strategy to mitigate the shuttle effect rather than physical confinement and thus realize high capacity and improved cycling performance.

Se/carbon

By controlling the process, researchers physically trap the active materials within the hosts with various structures, specific surface areas, and morphologies. Compared to pure Se, composites of Se and conductive hosts can be synthesized with prepared morphologies and works well. It is the most commonly used strategy to confine Se within carbon hosts because of their controllable structure, low cost, and high electronic conductivity and thermodynamic stability. By modifying carbon materials, expansion can be limited, and conductivity can be improved, although capacity may decrease.

Because of the strong interaction between the Sen molecule and CMK-3, Yang *et al.* added Se_8 molecule to ordered mesoporous carbon (CMK-3), which improved the stability of the battery and weakened the shuttle effect[32]. Ab initio calculations[Figure 12] further revealed that the order of binding energy between different selenides and the carbon host is Li_2Se_6 (-2.26 eV) > Li_2Se_4 (-2.07 eV) > Li_2Se (-1.44 eV)[64]. The combination of long-chain polyselenium with carbon host is preferred over that of short-chain polyselenium. Because of the chemical bond and physical packaging of carbon, the strong interaction between the carbon host and active material prevents the loss of Se and traps the polyselenides. Furthermore, the host enables the improvement of the mechanical stability and conductivity of cathodes[65-67].

Porous carbon has been widely used to encapsulate active material[19,68-76]. While the porous structure is able to store active material and inhibit the dissolution of polyselenides, the conductive network can serve as excellent electron/ion channels, and the stable and flexible matrix can buffer the volume change. By loading Se in layered mesoporous carbon spheres (MPCS), the sample size is uniform [Figure 13A and B], and the

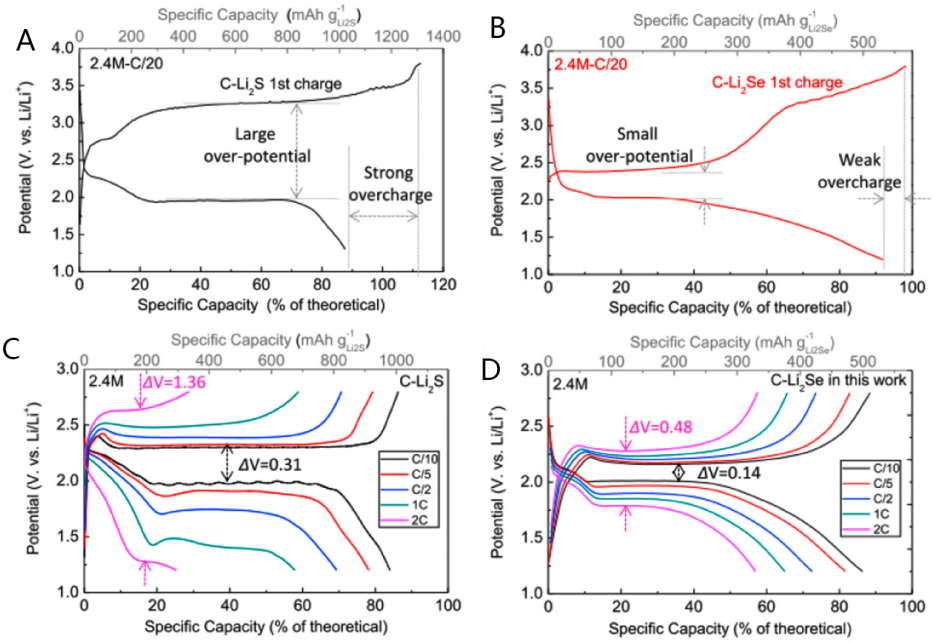

Figure 10. Comparisons of C-Li_2Se and C-Li_2S cathodes: (A and B) first charge-discharge profiles at C/20, (C and D) charge-discharge profiles recorded at different C rates[53]. Copyright 2016, Elsevier.

Se loading is also very uniform [Figure 13C], showing good rate performance and cycling performance [Figure 13D and E]. Remith *et al.* used hollow carbon spheres (HCSs) as Se cathode carriers for rechargeable Li-Se batteries [Figure 13J][77]. The Se@200HCS, as a cathode, has a capacity of 400 mAh/g and can last for 400 cycles [Figure 13I]. It also shows considerable capacity [Figure 13K] at a high magnification of 2 C. Luo *et al.* synthesized Se-impregnated carbon composite materials[31]. The mesoporous carbon injected with Se is spherical and has a smaller particle size [Figure 13F and G]. Homogeneous hollow carbon microspheres formed by Se impregnation have excellent cycling and rate performance in Li-Se batteries. [Figure 13H and I] This unique carbon framework can be used as conductive and polyselenide mediums due to its high surface area and porous properties.

In order to better accommodate Se molecules, the pore size should be larger than 1nm, but very large pores are unable to trap Se tightly. As evidence, Se-loaded carbon microspheres have well-developed micropores and mesopores(A4-carbon), exhibiting 582 mA h/g at the 500th cycle at 0.5 A/g, higher than that of Se-loaded carbon microspheres with only micropores (P-carbon/Se)[73]. Besides, the A4-carbon/Se exhibits stable reversible capacity after 2,000 cycles. The hierarchical structure helps fast conversion of Se_n in the cathode. Properties of Se/C cathode depend on its pore size and volume and Se content. Microporous carbons (MPC) show a volume confinement effect effectively, but hosts with both microporous and mesoporous work better[78,79].

When introducing Se into micro-MPCS (Se/MPCS), the smaller micropores completely disappear, while the mesopores are retained. Driven by capillary force, Se prefers to be adsorbed in the micropores than mesopores[19]. Another MPC is synthesized by carbonization of polyvinylidene fluoride (PVDF)[71]. When Se content increases from 50 wt% to 70 wt%, the specific and rate capabilities of MPC/Se decrease. As shown in Figure 14, the massive Se distributed on the carbon surface blocks the diffusion of Li-ions in micropores.

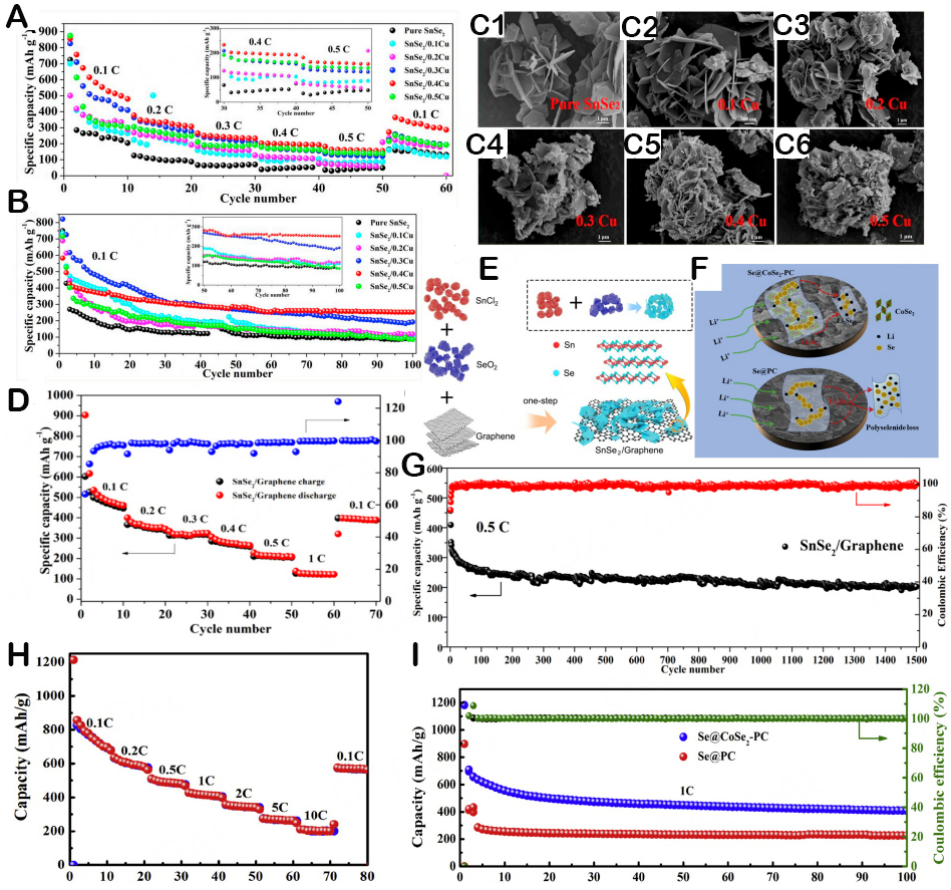

Figure 11. (A) Rate performance of pure $SnSe_2$ and five groups of Cu-doped $SnSe_2$ electrodes at various current densities (0.1, 0.2, 0.3, 0.4, 0.5 C). (B) Cycle performance at 0.1 C for 100 cycles, (C_1) SEM images of pure $SnSe_2$, (C_2) $SnSe_2$/0.1Cu, (C_3) $SnSe_2$/0.2Cu, (C_4) $SnSe_2$/0.3Cu, (C_5) $SnSe_2$/0.4Cu, (C_6) $SnSe_2$/0.5Cu[57], Copyright 2019, Elsevier. (D) Rate performance of 2D/2D $SnSe_2$/graphene heterostructure, (E) The synthesis and assembly process of 2D/2D $SnSe_2$/graphene heterostructure, (G) Long-term cycling performance at 0.5 C for 2D/2D $SnSe_2$/graphene heterostructure[59], Copyright 2020, Elsevier. (F) Illustration of the discharge process in Se-based cathodes, (H) Rate performance of the Se@$CoSe_2$-PC at increasing current density from 0.1 C to 10 C, (I) Cycling performance and coulombic efficiency comparisons between the Se@$CoSe_2$-PC and the Se@PC composite electrodes at 1 C[63]. Copyright 2018, Elsevier.

Hence, porous carbons with varied structures or morphologies appear to be hosts of active material. Such as plate[80], nanorod[81], sphere[82-84], hollow structure[77,85-87] and core/shell structure[88-90], as shown in Figure 15. For example, when microporous carbon spheres (MiPCS) are used to load Se[29], Se/MiPCS provides a capacity similar to the theoretical value of Se, showing 100% utilization of active material at 0.5 C, the capacity retains up to 515 mA h/g even after 100 cycles. Se/porous carbon nanospheres (PCNs) confine Se into PCNs[82]. The Se load can achieve as high as 70.5 wt%, and it shows excellent cycling stability in more than 1,200 cycles.

The hollow structure of carbon spheres realizes the effective and high-speed utilization of Se while maintaining the integrity of the structure to resist volume changes. Hollow and nonhollow selenium/nitrogen-containing carbon spheres (Se/NCS) exhibits 344 and 231 mA h/g, respectively[83]. Benefiting from the high conductivity and confinement of hollow spheres, the hollow carbonized polyaniline spheres/selenium (HCPS/Se) cathode exhibits a discharge capacity of 571.5 mA h/g, and after 100 cycles, it still maintains 298.7 mA h/g, which is higher than the discharge capacity of the original Se cathode[87].

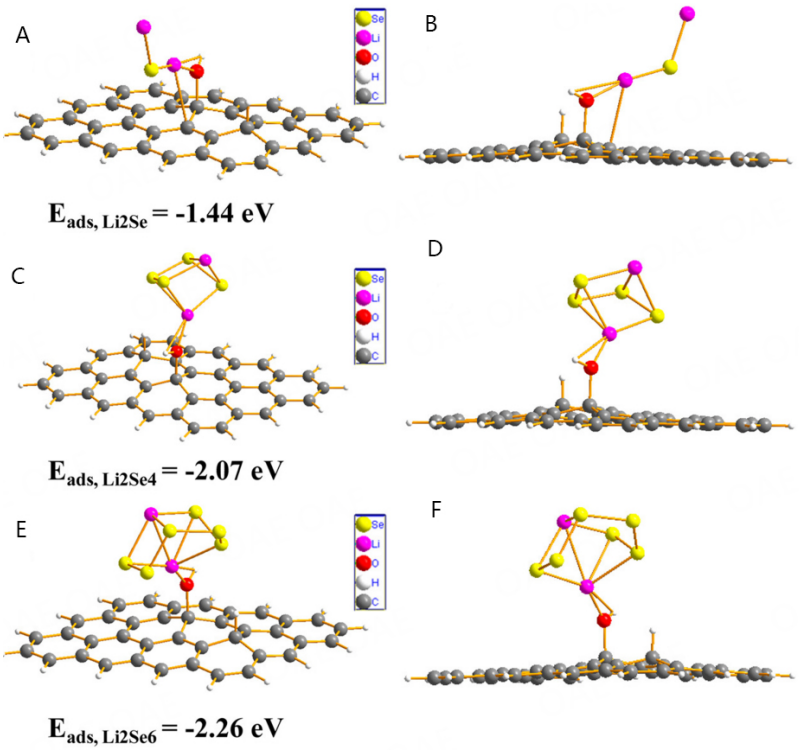

Figure 12. Ab initio calculations on the binding energy of different polyselenides with carbon host: (A and B) Li_2Se, (C and D) Li_2Se_4, and (E and F) Li_2Se_6 [64]. Copyright 2016, American Chemical Society.

For core-shell composites, the outer carbon shell not only provides electronic conductivity but also confines active material as a nanoscale capsule. Thus, the unique core-shell structure can effectively inhibit the dissolution of polyselenides into the electrolyte and maintain the high utilization rate of active materials[88]. Kalimuthu *et al.* developed another hollow N-containing carbon sphere (NHCS) with a mesoporous shell[89]. The unfilled mesoporous on the shell cushion the volume changes, realizing the longer cycle life. Remarkably, NHCS/Se cathode maintains an initial capacity of 75% at a rate of 2 C.

The introduction of novel carbon materials is a new way to improve the performance, such as carbon fibers[91-94], carbon nanotubes (CNTs)[95-97], and graphene[98-107]. N-doped carbon tubes (N-CT) work as carbon matrices for conducting and confining. The bimodal porous carbon nanofibers loaded with Seselenium achieved high capacity and excellent rate performance[Figure 16].

Graphene is widely used as a precursor or additive to take advantage of its excellent electrical conductivity. Graphene provides excellent specific surface area due to its excellent layered structure, providing more space for Se loading. By using graphene for loading, higher Se loading and better performance can be achieved. The 3D graphene-CNT@Se aerogel [as shown in Figure 17A] has an interlayer and conductive network, providing good channels for electron and ion migration[98]. In the absence of polymetallic adhesives, metallic current collectors, or conductive additives, the independent cathode shows high capacity. By embedding Se/MCN (mesoporous carbon NPs) in graphene sheets, a 3D hierarchical architecture is constructed[103]. Graphene matrixes provide high ionic and electronic conductivity, while graphene sheets accommodate the volume change and absorb the escaped polyselenides. The freestanding Se/MCN-RGO achieves high capacity and ultra-long cycle life. Rivera *et al.* used holey graphene to prepare cathodes with ultra-high Se content (up to 90 wt% Se) and ultra-high Se mass loadings

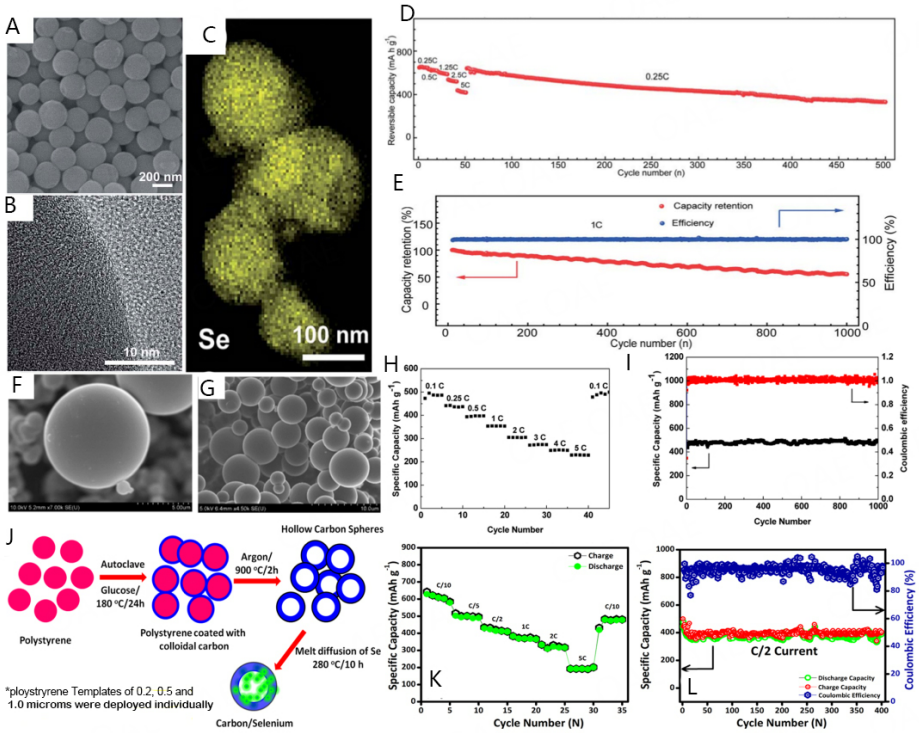

Figure 13. (A) SEM image of the Se/MPCS composite, (B) HRTEM image of the Se/MPCS composite, (C) elemental mapping of selenium before the test, (D) Rate capability of Se/MPCS composites in a lithium half-cell, (E) Cycling performances of the Se/MPCS-NMC full cell at 1 C[19], Copyright 2014, The Royal Society of Chemistry. (F) SEM images of Se/C composite and (G) mesoporous carbon spheres, (H) Rate capability of the Se/C composite, (I) Cycling performance of the Se/C composite[31], Copyright 2013, American Chemical Society. (J) Synthesis protocol designed to obtain hollow carbon spheres, (K) Rate capability of Se@HCS200 cathode, (L) Cycling performance of Se@HCS200 cathode[77]. Copyright 2019, American Chemical Society.

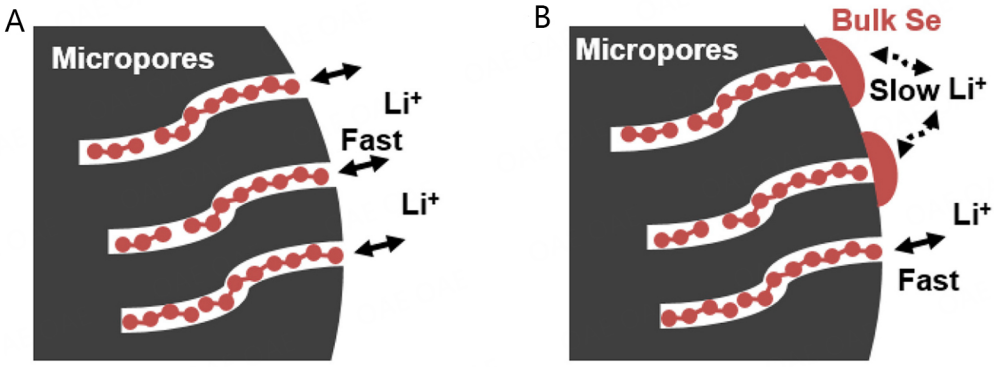

Figure 14. Schematics of (A) MPC 800/Se 50 and (B) MPC 800/Se 70[71]. Copyright 2019, Elsevier.

(up to 15.6 mg cm^{-2})[108]. These cathodes exhibit excellent Se utilization, high area capacity, and good rate performance. Therefore, using graphene with a higher specific surface area and unique structure can exhibit higher Se loading and utilization[108,109].

Excellent properties can be further obtained by controlling the particular structures of hosts, such as the hollow double-shell structure of the graphene-like laminar structure of Se/NCSs[100], 3D hierarchical selenium/carbon nanotubes and graphene (Se/G-CNTs)[104], graphene encapsulated sellenium/carboxylated

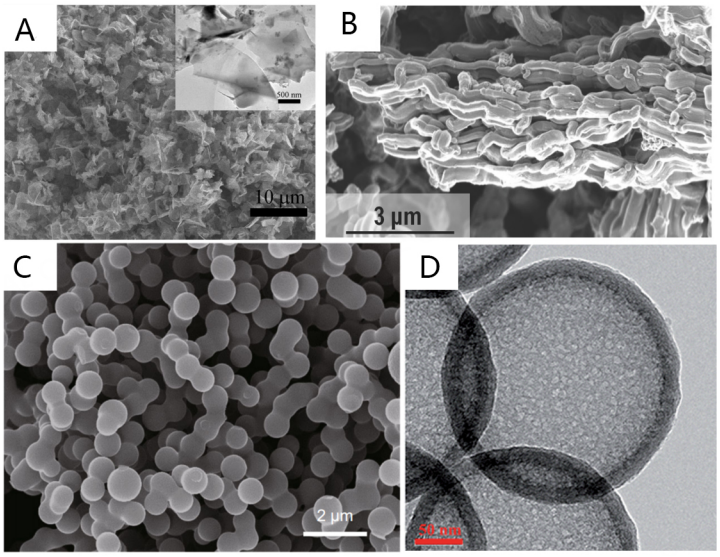

Figure 15. Porous carbon (A) nanoplate[80] Copyright 2018, Elsevier. (B) nanorod[81] Copyright 2014, Wiley-VCH. (C) sphere[29] Copyright 2015, Science China Press and Springer. (D) hollow sphere[86]. Copyright 2014, The Royal Society of Chemistry.

carbon nanotubes (Se/CCNTs-RGO)[105], and CN_x nanobelts[110] for Se encapsulation, fast ion transportation or space of volume variation, and so on. Except for commercial chemicals, carbons can be produced from various sources, especially biomass[111-117]. As shown in Figure 17B, the corncob-derived porous carbon (CPC) was obtained through KOH activation and carbonization. Se is uniformly distributed in the sponge-like carbon matrix, with high reversible capacity and almost no loss of coulombic efficiency[111].

Se/polymer

Conductive polymers (polypyrrole, PAN, PANI, *etc.*) tend to have electrical conductivity, unique chain structures, and flexibility, which is likely to improve the electrochemical performance of Se cathode. For example, PAN is considered one of the most attractive hosts due to its high reactivity with S compounds (including Se, S, and Te).

Se nanowires are sealed in the PANI layer at low temperature using the *in-situ* chemical oxidation polymerization method[41]. The G@Se/PANI core-shell nanowires exhibit better cycling performance and rate performance, as the PANI shell can greatly improve electronic conductivity and suppress the destruction of the electrode structure. Conducting polymer polypyrrole is coated on the Se nanofibers through surfactant-free solution processes[118]. Compared with a pure t-Se electrode, the Se/polypyrrole electrode exhibits smaller polarization between discharge and charging voltages. The use of polypyrrole can suppress the voltage hysteresis, suggesting faster electrochemical reaction kinetics. Otherwise, functional groups of polymers (such as N, amino, carbonyl, and carboxyl) could have strong interaction with polyselenides and thus inhibit their dissolution.

Se/metal compound

The porous metal oxide is another absorbing material as the polarity, which enhances the chemical trapping of Se and polyselenides, while the porous matrix provides physical confinement. For example, a TiO_2-Se composite cathode, with good dispersion of Se and good adsorption of polyselenides in the porous TiO_2, is competitive for long-life Li-Se battery[119]. Moreover, TiO_2 and Se are in close contact. This reduces the resistance of electron transfer through the interface between them.

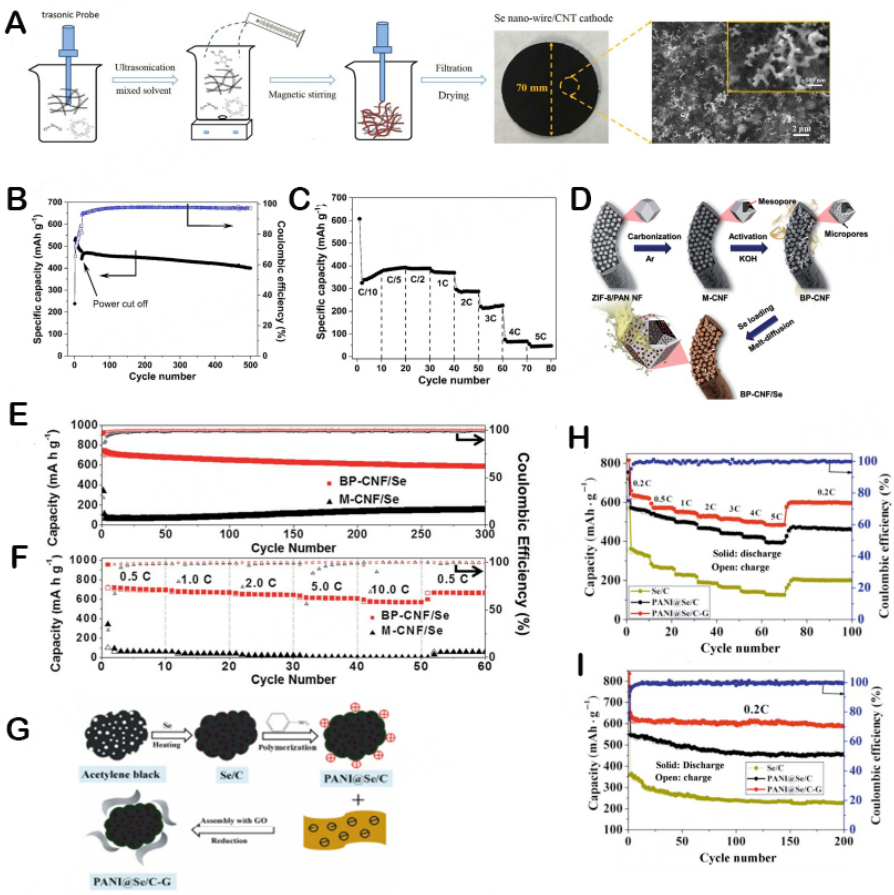

Figure 16. (A) Experimental procedure for the synthesis of the selenium nanowire/CNT composite electrode, with the SEM image showing the morphology of the composite electrode, (B) Cycling performance of the TSeCE at 1 C rate, (C) Rate performance of the TSeCE[97], Copyright 2019, Wiley-VCH. (D) Formation mechanism of bimodal porous nitrogen-doped carbon nanofiber homogeneously filled with chain-like Se, (E) cycling performance of BP-CNF/Se and M-CNF/Se at a current density of 0.5 C, (F) Rate performances with the coulombic efficiencies[91], Copyright 2018, The Royal Society of Chemistry. (G) Schematic illustration of the formation of the PANI@Se/C-G composite, (H) Rate capability at various current densities between 1.0 and 3.0 V for Se/C, PANI@Se/C, and PANI@Se/C-G, (I) Cycle performance at a current density of 0.2 C between 1.0 and 3.0 V[101]. Copyright 2017, Tsinghua University Press and Springer.

Metal organic frameworks (MOFs) used on Se carriers require high porosity, large specific surface area, high stability, and adjustable functionality[120-123]. The sandwich-like structure obtained in UIO-67@Se@PANI is effective in being a support matrix to host Se [Figure 18][121]. Moreover, the non-carbonized Zr-MOFs provide unsaturated sites to tether Se and polyselenides, and the PANI coating promotes electrical conductivity of the whole cathode, leading to high utilization of Se, better cycling stability, and improved rate capability.

Heteroatom-doped Se-based materials

The introduction of heteroatoms (e.g., B, S, N, P, and O) can bring many polar sites, which have a strong affinity for charged Se species and can significantly inhibit the shuttle effect and side reactions related to electrolytes. At the same time, the rich active sites are also conducive to accelerating Li-ion transport and electronic conductivity. Thus, heteroatom doping is a worthwhile method for Se-based cathodes to suppress the shuttle effect and boost the cycling lifespan.

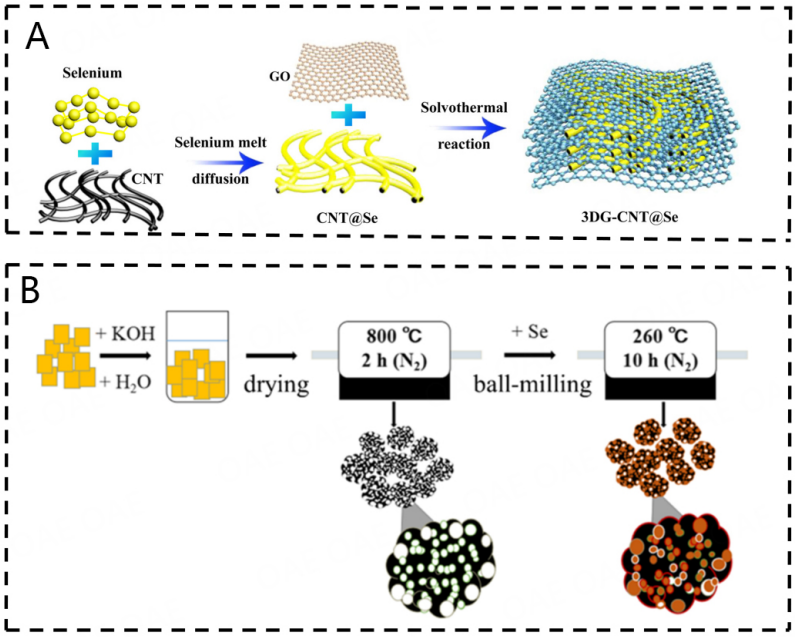

Figure 17. Schematic illustration of the synthesis procedure of (A) 3DG-CNT@Se composite[98], Copyright 2016, American Chemical Society. (B) Se/CPC[111]. Copyright 2022, Springer.

N, as an element next to C in the periodic table, is typically used to take the place of C in carbon-based composites. The Se/nitrogen-doped core-shell structure hierarchical porous carbon (Se/N-CSHPC)-II electrode exhibits outstanding Li-ion storage performance and minimal capacity degradation after 200 cycles at 1 C[120]. During the lithiation, the formed Li_2Se is adsorbed by N-doped graphite carbon, especially by the pyridinic N and pyrrolic N atoms. Together with the improved electrical conductivity, the reaction kinetics of Li^+/e^- are strengthened. The heteroatoms (N and O) doped in Se/heteroatoms dual-doped hierarchical porous carbon (Se/HDHPC) not only anchor the Se-contained species strongly but also help to tailor the electronic structure and fasten electron transfer[124]. Thus, Se/HDHPC cathode delivers a capacity of 613 mA h/g and low-capacity decay. In addition, even at 20 C, it exhibits excellent rate performance.

In various cathode materials, pure Se usually needs host materials with good conductivity, which can alleviate volume expansion and inhibit the diffusion of polyselenide due to poor expansion and conductivity. Due to the combination of their respective advantages, Se_xS_y cathodes have developed into one of the main research directions for Li-Se batteries. Li_2Se can be matched with Li-free anodes (such as metal oxides and silicon), which is expected to bypass the issues related to Li anodes. Amorphous carbon, CNTs, graphene, graphite, and other forms of carbon have unique structures and properties. Many works have verified the remarkable advantages of carbon-based hosts, which are expected to solve the shuttle and side reactions of polyselenide. Heteroatom doping also brings superior performance due to the introduction of many polar sites.

ANODE MATERIALS OF LI-SE BATTERIES

Li metal-based materials

The high theoretical capacity and low electrochemical potential have made Li metal the most commonly used anode material for high-energy batteries[17,18]. Thus, most of the Li-Se studies use Li metal foils as anodes,

$$Li \leftrightarrow Li^+ + e^- \quad (10)$$

In fact, the application of Li metal in rechargeable batteries is hindered by its high reactivity in the electrolyte and the infinite volume change in the cycling process. The reasons for the potential safety hazard, poor cycle stability, and low coulomb efficiency of Li-Se batteries are metal corrosion and the formation of dendrites on the surface of Li anodes.

Besides, alloys can be integrated into the system for better performance. Using the Li-Sn alloy as the anode, a fully solid Li-Se battery is displayed, which makes the anode/electrolyte interface more stable and provides the stable cycling performance. The use of solid electrolytes also prevents dendrite propagation[25,125]. Given the similarity with Li-S batteries, the anode protection and modification of Li-Se batteries can be adopted analogously, including insertion of the interlayer, modified diaphragm and electrolytes, and use of an artificial protective layer, and so on[16,126]. The revival of Li metal is on its way.

Li metal-free materials

As a container to store Li^+, Li metal is not necessarily used in the anode. It is a strategy to replace it with alternative anode materials not containing metallic Li. MXenes are a type of transition metal carbide/carbonitride materials with a 2D structure, exhibiting excellent ability in reversible embedding of many metal cations. Together with excellent mechanical properties, metallic conductivity, and hydrophilic surfaces, MXenes show their potential as promising electrode materials[127]. Theoretically, Se-terminated Ti_3C_2 MXenes can provide a low open circuit voltage (OCV) of 0.51 V and a capacity of 329.32 mA h/g due to double-layer Li-ion adsorption. The calculated result of Li-ion adsorption and migration in the $Ti_3C_2Se_2$ electrode is displayed in Table 2. It implies that high energy density can be obtained by coupling $Ti_3C_2Se_2$ MXene anode with a high redox potential cathode. In addition, $Ti_3C_2Se_2$ MXene shows excellent conductivity after maximum Li adsorption[128]. When compared with those of V_2CX_2 (X = O, S, and Te) monolayers, the single-layer V_2CSe_2 exhibits higher Li capacity and a small volume expansion, which means they may be a good choice for LIB anodes[Figure 19][129]. In addition, Li silicon is also a promising Li-free metal anode. By using Li silicon, the dissolution of intermediate products and unnecessary side reactions can be prevented, and the formation of Li dendrites can be avoided to improve the stability of LIBs.

Combining the Se/MPCS anode with the layered cathode ($LiNi_{1/3}Mn_{1/3}Co_{1/3}O_2$), a new Li-ion full battery exhibits good security, high capacity (660 mA h/g), and a long lifespan (1,000 cycles)[19]. Eom *et al.* used Li silicon as the anode, and the replacement of the anode prevented the side reaction between the Li metal and the intermediate products from the SeS_2 cathode and eliminated the formation of Li dendrites[130]. Therefore, the Li silicon/graphene SeS_2 full battery exhibits high capacity and long cycle stability, with a high-capacity retention rate. The Li-Se battery is a new study that has just been developed in recent years, and researchers are likely to concentrate more on the improvement of anodes in the future.

Although Li-based materials have higher theoretical capacity, they also have many problems, such as volume changes during cycling, poor stability, and the formation of surface dendrites. Li-free materials have low capacity, but materials such as MXenes have excellent mechanical properties, metal conductivity, and low expansion rates. Without metallic Li, Se-based electrodes still provide energy storage through a similar electrochemical reaction between Se and Li^+ of Li-Se batteries.

COMPONENTS OF LI-SE BATTERIES

Separator and interlayer

As the intermediate layer between the electrodes, the separator acts as an electron insulator to prevent

Table 2. The calculated adsorption energy (E_{ab}) of Li-ions on the surface of $Ti_3C_2Se_2$ in the most energy-favorable sites. Δq and Δh indicate the average charge transfer from the Li atom to $Ti_3C_2Se_2$ and the adsorption height of Li-ion on the $Ti_3C_2Se_2$ surface, respectively [128].

Structure	E_{ab} (eV)	Δq (e)	Δh (e)
$Ti_3C_2Se_2$	-1.11	0.25	1.56

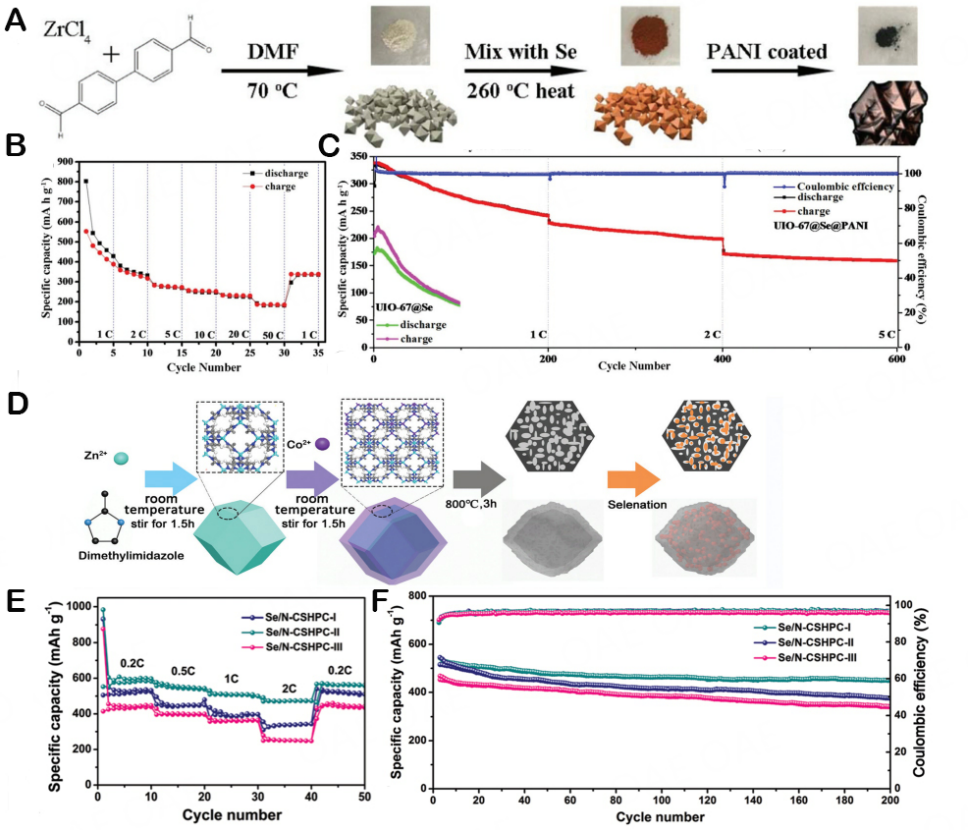

Figure 18. (A) Illustration of the synthesis process of the UIO-67@Se@PANI composite; (B) Rate performance text of the UIO-67@Se@PANI cathodes; (C) Cycling performances of the UIO-67@Se@PANI cathodes[121], Copyright 2019, The Royal Society of Chemistry; (D) Schematic illustration of the synthesis of the Se/N-CSHPC composite; (E) The rate performance of the Se/N-CSHPC electrodes at various current densities from 0.2 to 2.0 C; (F) The cycling performances of the Se/N-CSHPC-I, Se/N-CSHPC-II, and Se/N-CSHPC-III electrodes at 0.5 C[120]. Copyright 2019, The Royal Society of Chemistry.

battery short circuits and an ion conductor to maintain mass transfer. Li-Se batteries use nanoporous polymer membranes produced by CELGARD company as the most frequently used separators. However, the soluble polyselenides can diffuse to the anode through the separator, and react with Li, causing the capacity attenuation. Therefore, it is logical to capture or retain the polyselenides by introducing functional separators or inserting interlayers between the separator and electrodes.

With a covalent organic framework (COF) and highly regular pores, DMTA(polymerization by 2,5-Dimethoxy-1,4-Dicarboxaldehyde and Tetrakis(4-aminophenyl)ethane)-COF-coated ceramic separator can inhibit the polyselenide shuttle and ensure that the redox process mainly takes place in the cathode area[131]. Adding a barrier layer between the cathode and the diaphragm can be achieved by coating a layer of graphene on a commercial polymer diaphragm[132]. Through this design, a high-performance Li-Se battery with high Se content can be realized.

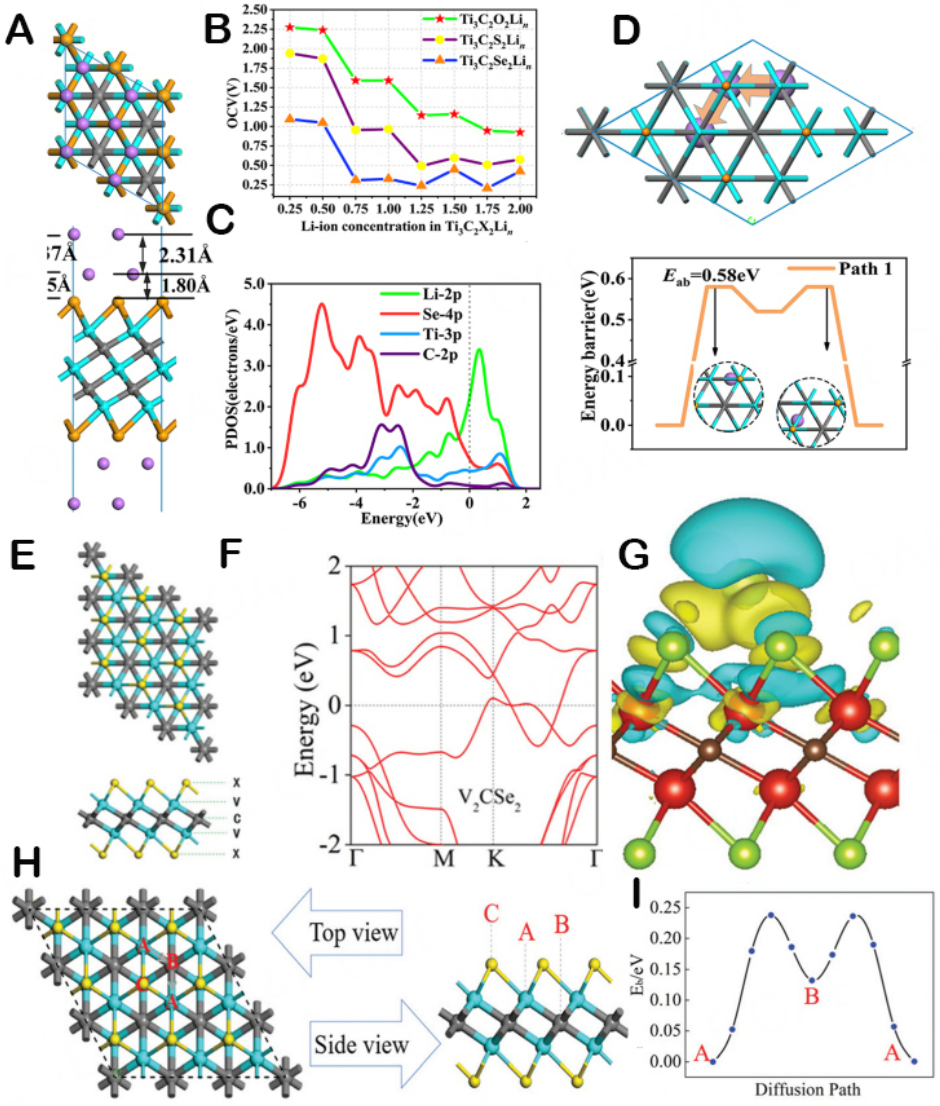

Figure 19. (A) Top and side view of the $Ti_3C_2Se_2$ with bilayer; (B) OCVs *vs.* Li-ion concentration, and (C) the partial density of states (PDOS) of $Ti_3C_2Se_2$, (D) Schematic illustration of the diffusion path of Li-ions in the double-deck $Ti_3C_2Se_2$. The corresponding energy profiles and the configurations of transition states (TS) are also provided[128], Copyright 2019, Elsevier. (E) Top view and side view of chalcogen-functionalized monolayer V_2CX_2 (X = S, Se, and Te), (F) Electronic band structures of monolayer V_2CSe_2, (G) The calculated difference charge densities of one Li-adsorbed monolayer V_2CSe_2, with isosurface 0.008 e/borh^3, the blue region represents electron depletion, while the yellow region represents electron accumulation,(H) Top view of three adsorption sites and the most favorable diffusion path upon the monolayer V_2CS_2, (I) Energy profile of the A -B - A path upon monolayer V_2CS_2 [129]. Copyright 2021, The Royal Society of Chemistry and the Chinese Chemical Society.

In order to better limit the polyselenides, a layer of CNTs was coated on the cathode side of the separator. Because of its conductive framework and cross-linked structure, the CNTs layer not only makes a good barrier to block the soluble discharge products but also supplies fast electron conduction and ion transport[104]. The conducting polymer poly(carbazon) PCZ coating layer[133], N,S-codoped graphene membrane[134], CPAN nanofiber membrane [Figure 20][135], and carbon interlayer based on carbonized cellulose filter paper[136] were adopted as the blocking layers for trapping polyselenides.

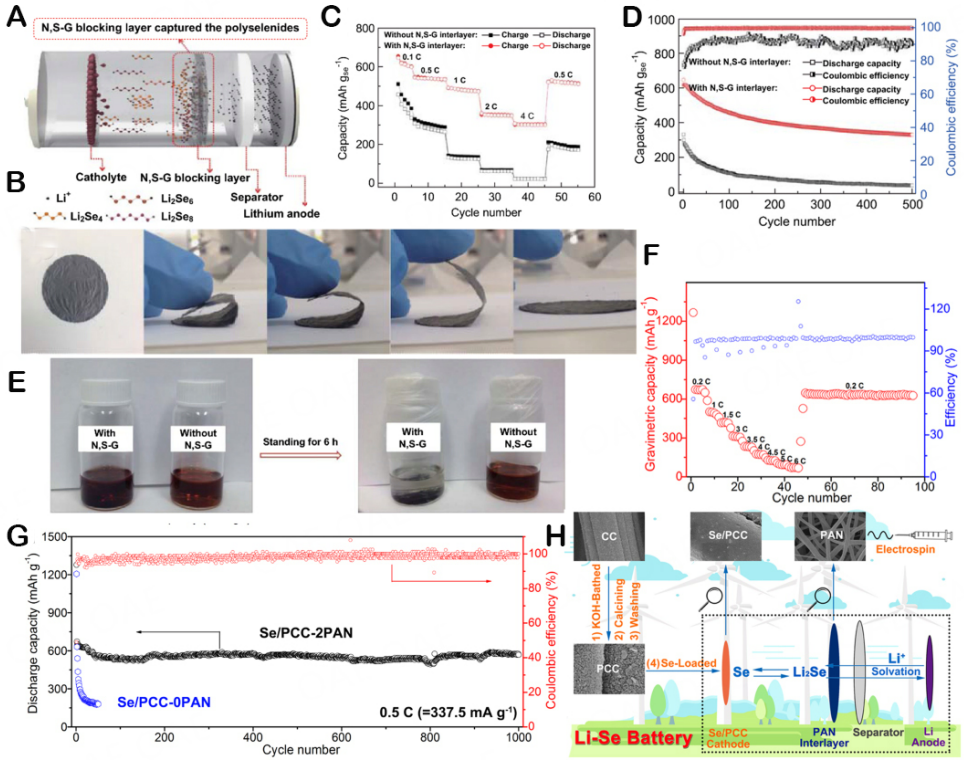

Figure 20. (A) N,S-G membrane as an interlayer for trapping polyselenides; (B) The freestanding N,S-G membrane; (C) Rate performance of Li-Se cells with and without N,S-G interlayer; (D) Long-term cycling performance of Li-Se cells with and without N,S-G interlayer; (E) Digital photographs of polyselenide adsorption by N,S-G interlayers[134], Copyright 2018, Springer. (F) Rate capability of the optimized Li-Se battery at various C-rates; (G) Cycling performances of the Se/PCC-2PAN and Se/PCC-0PAN systems at 0.5 C; (H) Preparation process for the Se/PCC cathode and PAN interlayer, and the brief model of the assembled Li-Se battery[135]. Copyright 2019, American Chemical Society.

Electrolyte

The electrolyte is an integral part of the battery because it helps to form an ion conduction path and combines with the external electronic path to form a closed loop[4]. Given the solubility difference of polyselenides in various electrolytes, some research aims to change the compositions of solutes or solvents.

The polyselenides have high solubility in liquid LiTFSITEGDME electrolytes, which can better realize the utilization of Se, thus increasing the capacity[31]. In ether-based electrolytes, the formation of soluble polyselenium promotes the transport of Li-ions and electrons but leads to the shuttle effect. In carbonate-based electrolytes, no shuttle effect is expected. There is no soluble polyselenide with cheaper carbonate-based electrolytes, so even good reversibility and long lifetime are achieved in several systems, but the electrochemical process is still relatively not fast enough[29,30,70]. It is found that when the molar concentration of electrolytes is high, the dissolution of Se is inhibited, and the capacity utilization rate is improved due to better electrons on the cathode entering the reaction center and higher Li mobility, excellent rate performance, and high-capacity utilization achieved in 5 M and 7 M electrolytes[81].

Organic liquid electrolytes usually cause serious safety problems and limited cycle life. The violent interaction between dissolved species and electrodes harms the stability and properties of batteries, which can be avoided by using solid electrolytes. Based on the Li_2S-P_2S_5 solid-state electrolyte, an all-solid-state Li-Se battery shows significant voltage distribution; it has a single platform, minimal voltage lag, and good cycle stability, which is due to the lack of dissolution of polyselenides[53]. All-solid-state batteries always

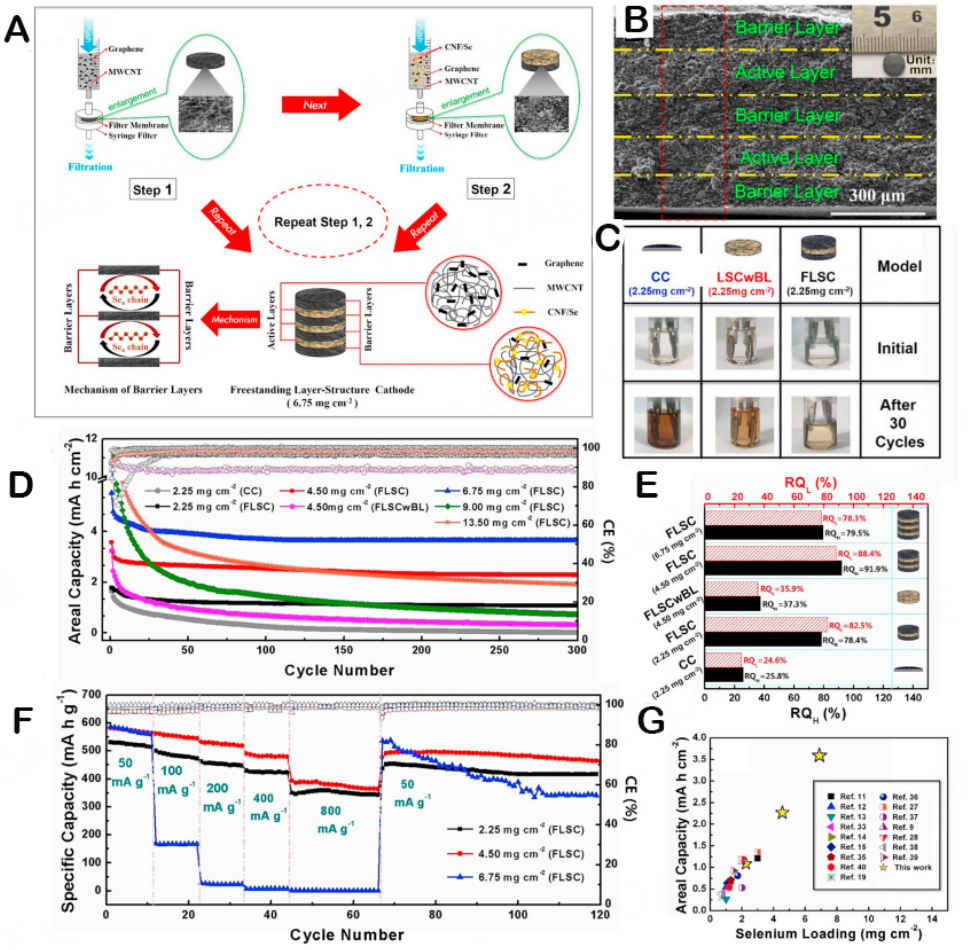

Figure 21. (A) Schematic illustration of the synthesis process of freestanding layer-structure Se cathode; (B) Cross-sectional SEM image of freestanding layer-structure Se cathode. The inset of (B) is a digital photo of a freestanding layer-structure Se cathode; (C) Digital images of different Se cathodes before/after 30 cycles; (D) Cycling performance of various Se cathodes under the current density of 50 mA g^{-1}; (E) RQH/RQL analyses of various Se cathodes; (F) Rate performance of freestanding layer-structure Se cathodes with different Se loadings; (G) Areal capacity comparison of various Se cathodes[140]. Copyright 2018, Elsevier.

suffer from poor Li^+ conductivity at the interface. However, by using Li_3PS_4 as the solid-state electrolyte, a higher Li^+ conductivity has been achieved at the Se-sulfide electrolyte interface[25].

By using all-solid-state Li-Se batteries, the safety of the battery can be significantly improved, as there will be no electrolyte leakage. The characteristics of Li metal anodes can also make the system have a high energy density, making it a potential energy storage system. But the fatal weakness of all-solid-state Li batteries is the poor Li^+ and electron transfer performance between the electrodes and electrolytes. Li *et al.* formed an all-solid-state Li-Se battery by using Li_3PS_4 electrolyte[25]. It achieved high electronic conductivity of Se and high Li+ conductivity at the Se-sulfide electrolyte interface. Afterward, researchers constructed solid-state Li-Se batteries based on the high ionic conductivity halide Li_3HoCl_6 as a solid electrolyte[137]. Because Li_3HoCl_6 has a wide intrinsic wide electrochemical stability window and good stability, it effectively inhibits the degradation of electrolyte and Se cathode by inhibiting side reactions, providing new insights for the development of future all-solid-state Li-Se batteries[138]. If we can solve the interface impedance-related issues in the future, we believe that all-solid-state Li-Se batteries with excellent safety and energy density will become an important component of the energy storage field.

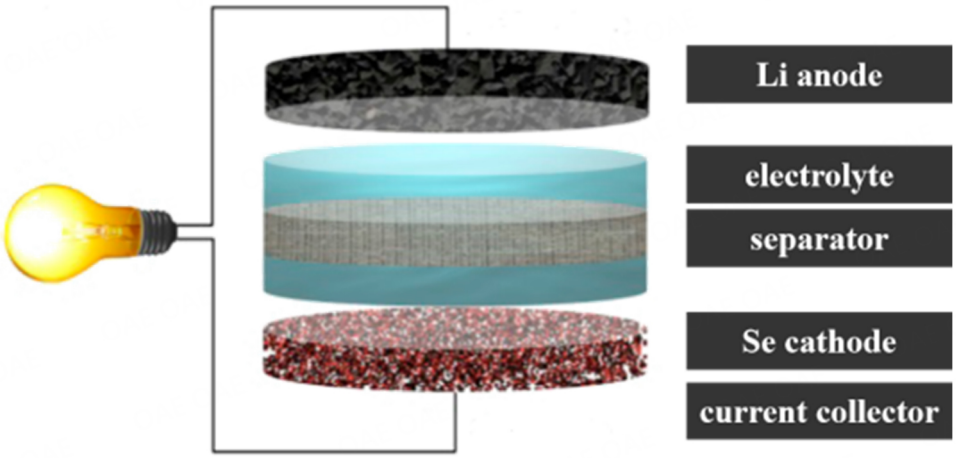

Figure 22. Schematic of the Li-Se coin cell.

Binder

In order to make active material particles in close contact with the current collector, a binder is needed to paste the Se cathode. As Se is insoluble in water but slightly soluble in N-methyl-2-pyrrolidone (NMP) and sodium alginate (SA), a stable water-soluble binder is selected to avoid Se dissolving in NMP. Compared with poly (vinylidene fluoride) (PVDF) binder (dissolved in NMP), Li-Se batteries with SA exhibit better electrochemical performance.

Actually, additional binder and conductive additives result in lower Se loading. It is worth exploring binder-free cathodes to increase the Se loading. Through magnetic stirring[97], vacuum-filtration[110], or thermal perfusion strategy with ultrasonication and vacuum filtration methods[106], binder-free cathodes can be prepared easily and show high capacity and stability. Huang *et al.* synthesize a freestanding cathode by galvanic replacement method, in which the Ni foam is used as both the collector and the base of Se without any adhesive[139]. Eliminating the use of adhesives can improve the kinetics of the reaction, especially the electrochemical performance at a high rate. Furthermore, after the morphology of the Ni substrate is changed, the preparation of Se with various structures can also be simplified, which will greatly affect the performance of the battery.

Current collector

The current collector with high conductivity and large active surface area can greatly enhance the transport and the electrochemical reaction of Li-ions and electrons. That is the reason why most studies adopted Al foil or foamed Ni. The barrier layer is composed of multi-walled CNTs (MWCNTs) and graphene, which are intertwined with each other and act as polyselenide-interception blocking layer and high conductive collector. The optimized Se cathode without a metallic current collector has strong polyselenide capture and fast redox conversion abilities [Figure 21][140]. Also, various current collectors are needed to increase the utilization rate of Se with high Se loading and suppress the Li dendrites.

ASSEMBLY AND INTEGRATION OF THE BATTERY

The produced active material powders are mixed with conductive additives and binder in an aqueous or nonaqueous solvent to form a slurry at a particular weight ratio for casting a cathode. Magnetically stir the slurry at room temperature for several hours until smooth and pasted evenly on the current collector. After drying, a sheet of the plate is cut into Se cathodes.

Together with electrodes, the electrolyte, separator, and current collector contribute to the overall performance of the system. When assembling cells using the prepared Se cathode, all components need to stay in an Ar-filled glove box. First, the Se cathode is placed into the metal shell of the coin cell. Then a separator is placed on the top of the cathode, followed by adding an electrolyte to the separator. A piece of Li foil as the anode is placed on the separator, then a steel sheet and a spring washer. Finally, the cell is covered and packed, as shown in Figure 22. After being equilibrated for 24 h, the Li-Se battery with the assembly of a coin cell can be taken out of the glove box for electrochemical evaluation.

CONCLUSION AND PERSPECTIVE

Se, with high volumetric specific capacity and relatively high conductivity, has received much attention in energy storage[141-150]. Although the Li-Se system is constrained by the shuttle effect and volume expansion, some corresponding measures and advice are proposed based on the analysis of the problems. Moreover, the detailed process and the mechanism should be further investigated. This review summarizes the performance of Li-Se batteries in recent years in Table 3.

We focus on optimizing methods, especially in terms of cathodes. By modifying carbon materials and metal compounds and doping with heteroatoms, the energy storage performance of cathode materials can be significantly improved. In addition to the morphology and size modifications of Se, the structure and composition designing of the active material is an effective method. In particular, the use of flexible hosts capable of withstanding the mechanical stress or mesh matrix to increase the Se loading and contact area enhances the kinetics, capacity, and stability.

All-solid-state Li-Se batteries are also a development idea. All-solid-state Li-Se batteries can fundamentally avoid the stubborn problems of Li-Se batteries involving parasitic reactions and the dissolution of polyselenide. In addition, their high thermal stability allows for a wider operating temperature and resistance to Li dendrite short circuits. Therefore, the design of future solid-state Li-Se batteries urgently requires solid-state electrolytes with low interface resistance and high ionic conductivity.

In addition, sodium (Na)-Se batteries are also a development direction. Many non-Li-Se batteries, including Na-Se batteries, have become promising substitutes for Li-Se batteries because of their abundant raw material resources and low manufacturing costs. They face similar challenges as Li-Se batteries, and the design strategy of Li-Se batteries is also applicable to these emerging battery systems. While the lessons of the Li-S system offer insight into the Li-Se system, the design of the Se cathode should explore its own way based on the very different nature rather than merely copy. The current changes in policies and the requirements of the ecological environment have prompted us to develop Li-Se batteries with high energy density, high cycle life, and high safety for future energy applications. This is very challenging.

At present, the main challenges of Li-Se batteries include low bulk Se reactivity, shuttle effect triggered by soluble polyselenide, rapid volume changes during electrochemical reactions, slow redox kinetics, slow diffusion rates of Li-ions in Se, and growth of Li dendrites. Most of these problems stem from Se positive electrodes, so it is very important to adopt appropriate positive electrode strategies to improve performance. The heteroatom doping strategy provides a way to enhance the overall performance of carbon by adjusting the material structure at the atomic level. However, further research is still needed in terms of doping sites, doping agent content, and configuration optimization.

Table 3. Performance of current lithium selenium batteries (1 C = 0.675 A/g)

Cathode	Synthesis	Electrolyte	Capacity (mA h/g)	Cyclability (mA h/g)	Note	Reference
$SeS_{0.7}$/CPAN	Annealed at 600 °C under vacuum	$LiPF_6$ in EC/DEC	900@60 mA/g, capacity retains 50%@6 A/g, recovers @60 mA/g	780@600 mA/g (1,200 cycles)	/	[46]
Se nanowires	Mechanical injection method	1.0 M $LiPF_6$ in EC/DEC	Initial: 1,425.6@150 mA h/g	258@150 mA h/g(50 cycles)	80 wt% of Se	[42]
Selenium/interconnected porous hollow carbon bubbles composites	Melt-diffusion method	1.0 M $LiPF_6$ in EC/DEC(1:1, v/v)		606.3(120 cycles)@0.1 C		[85]
G@Se/PANI	Situ chemical oxidative-polymerization	1.0 M $LiPF_6$ in EC/DEC	510.9@2 C	567.1@0.2 C (200 cycles)	Core-shell nanowires	[41]
Polyaniline (PANI)-coated selenium/carbon nanocomposite encapsulated in graphene sheets (PANI@Se/C-G)	Melt-diffusion method, *in-situ* oxidative polymerization method, and electrostatic interactions	1.0 M LiPF6 in EC/DEC (1:1 , v/v)	628.1@0.2 C	588.7 (200 cycles)@0.2 C, 528.6 (500 cycles)@2 C		[101]
Selenium@Mesoporous Carbon Composite	Infusion at 600 °C under vacuum	1.0 M $LiPF_6$ in EC/DEC	480@0.25 C	1,000 cycles without any capacity loss		[31]
Se@RGO	Two-step solution process	1.2 M $LiPF_6$ in EC/DEC	Initial: 543@0.2 C	343@0.2 C (50 cycles)	70 wt% of Se	[107]
$NiSe_2$ thin film	Reactive pulsed laser deposition at 200 °C	1.0 M $LiPF_6$ in EC/DMC	315	467.5 to 314.9 (200 cycles)@5 μA/cm^2		[62]
Sb_2Se_3 thin film	Reactive pulsed laser deposition at 200 °C	1.0 M $LiPF_6$ in EC/DMC	605.1	660.7 to 530.5 (100 cycles)@5 μA/cm^2		[60]
$CuInSe_2$ thin film	Pulsed laser deposition	1.0 M $LiPF_6$ in EC/DMC	555	438 to 647 (100 cycles)@5 μA/cm^2		[142]
Se/porous carbon nanospheres (PCNs) composite	Hydrothermal route and melting-diffusion	1.0 M $LiPF_6$ in EC/DMC (1/1, v/v)	Volumetric capacity of 3,150 (780 for the composite) mAh /cm^3 @1 C	Over 1,200 cycles with a capacity decay as low as approximately 0.03% per cycle	Se loading is 70.5 wt%	[82]
Cu-doped $SnSe_2$ nanoflakes composites	Hydrothermal method	1.0 M $LiPF_6$ in EC/DMC		583 to 254 (100 cycles)@0.1 C	$SnSe_2$/0.4Cu	[57]
Trigonal Selenium nanofibers and t-Se/-polypyrrole, t-Se/-graphene composites	Solution processes	1.0 M $LiPF_6$ in EC/DMC	678 Ah/kg (pure t-Se fibers)@C/120; 375 Ah/kg (t-Se/-graphene)@C/13			[118]
Selenium/micro-mesoporous carbon sphere nanocomposite (Se/MPCS)	The hydrothermal process combined with the KOH activation	1.0 M $LiPF_6$ in EC/DMC (1:1 wt%)	660@0.1 C; 430@5 C	Long lifespan of 1,000 cycles		[19]
Se/CNFs-CNT	Heating Se with carbon nanofibers-CNT	1 M$LiPF_6$ in ethylene carbonate-dimethyl carbonate (W_{EC}:W_{DMC} = 1:1)	950@0.5 A/g	638 (80 cycles)@0.05 A/g, 517 (500 cycles) @0.5 A/g		[94]
Nanoporous Se	A simple mechanical method	1.0 M $LiPF_6$ in EC/DMC /DEC	338@100 mA/g	206@100 mA/g (20		[40]

	adopting nano-$CaCO_3$ as a template			cycles		
A-Se NWs and c/a-Se NWs	A facile ball milling process and the following sintering at 80 °C	1.0 M $LiPF_6$ in EC/DMC /DEC	755 and 705@0.1 C	/	/	[141]
Self-standing grapheneeSe@CNT composite film	Thermal infusion strategy, ultra-sonication, and vacuum filtration approach	1.2 M LiPF6 in EC/EMC (3:7, v/v)	400@0.1 C	315 mAh/g (100 cycles)@0.1 C	Without extra binders and conductive additives	[106]
Li/Se-C; Li/SeS_2-C	High energy ball milled and heated at 260 °C under air	1.2 M $LiPF_6$ in EC/EMC	Sustain 500@10 mA/g, reduce to 300@50mA/g for 100 cycles (Se)	394 (Se) 512(SeS_2) @50 mA/g (30 cycles)	280@10 0 mA/g (Se, 80 cycles)	[11]
Se@$CoSe_2$-PC	Co-PC in one-pot reaction and $CoSe_2$ in melt-diffusion	1.0 M $LiPF_6$ in EC/EMC/DMC/		408 (100 cycles)@1 C	$CoSe_2$ served as an effective electrocatalyst	[63]
Se/HPCF-rGO	Electrospinning technique, melt diffusion method, solvothermal reaction	1 M LiPF6 in a mixture of EC/EMC/DMC with a mass ratio of 1:1:1		616 mA h /g (50 cycles)@0.2 C, 208 mAh/g (5,000 cycles) @10 C		[102]
Microporous carbon confined Se cathode (Se/MC)	Embedding Se into a metal organic framework derived microporous carbon	LiDFOB/EC-DMC-FEC electrolyte	569 mA h/g@20 C, 94.4% of that @0.5 C (603 mA h/g)	511 (1,000 cycles) mA h/g@5 C		[146]
CMK-3/SeS_2@PDA	Filling SeS_2 within CMK-3 by melt-diffusion and coating PDA sheath	1 M LiTFSI and 0.2 M LiNO3 in DOL/DME	1,234@0.2 A/g; 535@5 A/g	350@2 mA/g (500 cycles)	70 wt% of SeS_2	[48]
Se_2S_5/MPC	A modified vaporization-condensation method	1.0 M LiTFSI in DOL/DME with 0.1 M $LiNO_3$ additive	691.9@0.5 C; 360@2 C to 5,000@1 C	430.2@0.5 C (100 cycles)	/	[64]
UIO-67@Se@PANI	/	1.0 M LiTFSI in DOL/DME (1:1 by volume) with a 1 wt% LiNO3 additive	248.3@0.5 C	203.1 (100 cycles)@2 C, 167.6 (100 cycles)@5 C		[121]
N-doped interconnected porous carbon nanofiber webs/selenium (PCNFW/Se)	Pyrolyzation of polypyrrole (PPy) nanofiber and a subsequent KOH activation	1 M LiTFSI in DOL/DME (1:1, v/v)	563.9@0.2 C	414.5 (100 cycles)@0.2 C; 323.7 (300 cycles)@1 C		[95]
Hierarchical porous carbon aerogels (HPCA)/Se	Sol-gel process, KOH etch and melt-diffusion	1 M LiTFSI in DOL/DME (1:1, v/v)	301@5 C	587 to 367 (50 cycles)@0.5 C	309 (100 cycles) in $LiNO_3$ modified electrolyte; CE > 92% in PYR_{14}TFSI modified electrolyte	[143]
Se@RGO	Self-assembly process	1.0 M LiTFSI in DOL/DME	533@0.2 C; 250@5 C	265@0.2 C (200 cycles) and 1 C (300 cycles)	80 wt% of Se	[39]
Mesoporous texture carbon (meso-C)@Se composite	Carbonizion of MOF-5 and melt-diffusion with Se	1 M LiTFSI in DOL/DME (1:1, v/v)	641@0.5 C;659.9@2 C	306.9 (100 cycles)@0.5 C; 279.5 (100 cycles)@2 C		[144]
TiO_2-Se composite cathode	Se melt-diffusion at 260 °C for 12 h	1 M bis(trifluoromethane) sulfonamide lithium salt in a mixed solvent of 1,3 dioxolane and 1,2-dimethoxyethane (volume ratio: 1:1)	481 mAh/g@0.1 C	158 mAh/g (50 cycles)@0.1 C		[119]

Se-nitrogen-containing hierarchical porous carbon (NCHPC)	A facile template route with gelatin as a precursor and silica spheres as hard templates	2 M LiTFSI in DOL/DME (1:1, v/v)	435@2 C	305 (60 cycles)@2 C		[75]
Se- bimodal porous carbon (BPC)	A facile hydrothermal route and KOH activation process	2 M LiTFSI in a solvent mixture of 1,3-dioxolane and 1,2dimethoxyethane (1:1, v/v)	552@1 C	264 (80 cycles)@1 C		[145]
C-Li_2Se; C-Li_2Se@C	Solution-based method (Li_2 Se-Polymer), carbonization (N-doped C-Li_2Se), and CVD (C shell)	Organic-liquid electrolytes and Li_2S-P_2S_5 -based solid-state electrolyte		310 (C-Li_2Se) 295(C-Li_2 Se@C)@C/2 (100 cycles)	All-solid-state Li-C-Li_2 Se@C/10:330 to 475 (60 °C, 50 cycles) and 488 to 579 (80 °C, 50 cycles)	[53]
Se/CMK-3 composite	A facile melt-diffusion process	Carbonate electrolyte	670 (2nd cycle)@0.1 C	600 (50 cycles)@0.1 C	Cathode is pasted with the SA binder	[32]
Se_nS_{8-n}/NMC	A facile melt-impregnation method	Ether-based electrolyte	High rate: 525@5 A/g	883 (100 cycles) and 780 (200 cycles)@250 mA/g	Se/S mole ratio = 2/6	[49]
Se/Porous hollow carbon spheres (PHCSs)	A facile template method		590@0.1 C	338 (50 cycles)@0.1 C		[86]

In addition to achieving stable and feasible Se positive electrodes, improving battery performance also requires initiating research on many aspects beyond the positive electrode. We expect that Li-Se batteries can be further optimized by selecting electrodes, appropriate electrolytes, and suitable separators. The use of Li-free anodes, binders (or even no binders), and current collectors is a vital part of reaching the overall performance as well. Li-Se batteries still have a long way to go in practical engineering, but the future is bright with new thinking and gradual improvements in battery designs.

DECLARATIONS

Author Contributions

Conceptualization, investigation, writing - revise and optimize the manuscript: Yang Z
Conceptualization, methodology, writing - original draft: Lu Y
Investigation, methodology: Wang Z, Dong H, Lin J, Wang Y, Qiu M
Supervision, project administration, funding acquisition: Ye Z
Conceptualization, writing - review & editing, supervision, project administration, funding acquisition: Lu J

Availability of data and materials

Not applicable.

Financial support and sponsorship
This work was supported by the "Pioneer" and "Leading Goose" R&D Program of Zhejiang Province (2023C01235).

Conflicts of interest
All authors declared that there are no conflicts of interest.

Ethical approval and consent to participate
Not applicable.

Consent for publication
Not applicable.

REFERENCES

1. Nitta N, Wu F, Lee JT, Yushin G. Li-ion battery materials: present and future. *Mater Today* 2015;18:252-64. DOI
2. Li M, Lu J, Chen Z, Amine K. 30 years of lithium-ion batteries. *Adv Mater* 2018;30:e1800561. DOI
3. Qi W, Shapter JG, Wu Q, et al. Nanostructured anode materials for lithium-ion batteries: principle, recent progress and future perspectives. *J Mater Chem A* 2017;5:19521-40. DOI
4. Zhang X, Zhao C, Huang J, Zhang Q. Recent advances in energy chemical engineering of next-generation lithium batteries. *Engineering* 2018;4:831-47. DOI
5. Whittingham MS. Lithium batteries and cathode materials. *Chem Rev* 2004;104:4271-301. DOI PubMed
6. Wu F, Yushin G. Conversion cathodes for rechargeable lithium and lithium-ion batteries. *Energy Environ Sci* 2017;10:435-59. DOI
7. Song L, Zheng T, Zheng L, et al. Cobalt-doped basic iron phosphate as bifunctional electrocatalyst for long-life and high-power-density rechargeable zinc-air batteries. *Appl Catal B* 2022;300:120712. DOI
8. Xu J, Ma J, Fan Q, Guo S, Dou S. Recent progress in the design of advanced cathode materials and battery models for high-performance lithium-X (X = O_2, S, Se, Te, I_2, Br_2) batteries. *Adv Mater* 2017;29:1606454. DOI
9. Cao Z, Zhang Y, Cui Y, Li B, Yang S. Harnessing the unique features of MXenes for sulfur cathodes. *Tungsten* 2020;2:162-75. DOI
10. Yang CP, Yin YX, Guo YG. Elemental selenium for electrochemical energy storage. *J Phys Chem Lett* 2015;6:256-66. DOI PubMed
11. Abouimrane A, Dambournet D, Chapman KW, et al. A new class of lithium and sodium rechargeable batteries based on selenium and selenium-sulfur as a positive electrode. *J Am Chem Soc* 2012;134:4505-8. DOI PubMed
12. Jin J, Tian X, Srikanth N, Kong LB, Zhou K. Advances and challenges of nanostructured electrodes for Li-Se batteries. *J Mater Chem A* 2017;5:10110-26. DOI
13. Gu X, Tang T, Liu X, Hou Y. Rechargeable metal batteries based on selenium cathodes: progress, challenges and perspectives. *J Mater Chem A* 2019;7:11566-83. DOI
14. Eftekhari A. The rise of lithium-selenium batteries. *Sustain Energy Fuels* 2017;1:14-29. DOI
15. Zeng L, Li W, Jiang Y, Yu Y. Recent progress in Li-S and Li-Se batteries. *Rare Metals* 2017;36:339-64. DOI
16. Tao T, Lu S, Fan Y, et al. Anode improvement in rechargeable lithium-sulfur batteries. *Adv Mater* 2017;29:1700542. DOI
17. Lin D, Liu Y, Cui Y. Reviving the lithium metal anode for high-energy batteries. *Nat Nanotechnol* 2017;12:194-206. DOI PubMed
18. Kim H, Jeong G, Kim YU, et al. Metallic anodes for next generation secondary batteries. *Chem Soc Rev* 2013;42:9011-34. DOI
19. Ye H, Yin Y, Zhang S, Guo Y. Advanced Se-C nanocomposites: a bifunctional electrode material for both Li-Se and Li-ion batteries. *J Mater Chem A* 2014;2:13293. DOI
20. Kotkata MF, Nouh SA, Farkas L, Radwan MM. Structural studies of glassy and crystalline selenium-sulphur compounds. *J Mater Sci* 1992;27:1785-94. DOI
21. Saji VS, Lee C. Selenium electrochemistry. *RSC Adv* 2013;3:10058. DOI
22. Murphy KE, Wunderlich BB, Wunderlich B. Effect of structure on the electrical conductivity of selenium. *J Phys Chem* 1982;86:2827-35. DOI
23. Itoh S, Nakao K. Electronic states in allotropes of sulphur and selenium-localised orbital approach. *J Phys C Solid State Phys* 1984;17:3373-89. DOI
24. Sangster J, Pelton AD. The Li-Se (lithium-selenium) system. *J Phase Equilibria* 1997;18:181-4. DOI
25. Li X, Liang J, Li X, et al. High-performance all-solid-state Li-Se batteries induced by sulfide electrolytes. *Energy Environ Sci* 2018;11:2828-32. DOI

26. Morachevskii AG. Lithium-selenium and sodium-selenium systems: thermodynamic properties and prospects for use in chemical current sources. *Russ J Appl Chem* 2016;89:1043-53. DOI
27. Liu F, Wang L, Zhang Z, et al. A mixed lithium-ion conductive Li_2S/Li_2Se protection layer for stable lithium metal anode. *Adv Funct Mater* 2020;30:2001607. DOI
28. Cui Y, Abouimrane A, Lu J, et al. (De)lithiation mechanism of Li/SeS_x (x = 0-7) batteries determined by in situ synchrotron X-ray diffraction and X-ray absorption spectroscopy. *J Am Chem Soc* 2013;135:8047-56. DOI
29. Wu C, Yuan L, Li Z, et al. High-performance lithium-selenium battery with Se/microporous carbon composite cathode and carbonate-based electrolyte. *Sci China Mater* 2015;58:91-7. DOI
30. Cui Y, Abouimrane A, Sun CJ, Ren Y, Amine K. Li-Se battery: absence of lithium polyselenides in carbonate based electrolyte. *Chem Commun* 2014;50:5576-9. DOI PubMed
31. Luo C, Xu Y, Zhu Y, et al. Selenium@mesoporous carbon composite with superior lithium and sodium storage capacity. *ACS Nano* 2013;7:8003-10. DOI
32. Yang CP, Xin S, Yin YX, et al. An advanced selenium-carbon cathode for rechargeable lithium-selenium batteries. *Angew Chem Int Ed* 2013;52:8363-7. DOI
33. Xu F, Qiu DR, Yang PY, et al. Review of chemical and biological speciation analyses for Se. *Spectrosc Spect Anal* 2002;22:331-40. DOI
34. Zhang J, Wang H, Yan X, Zhang L. Comparison of short-term toxicity between Nano-Se and selenite in mice. *Life Sci* 2005;76:1099-109. DOI
35. Painter EP. The chemistry and toxicity of selenium compounds, with special reference to the selenium problem. *Chem Rev* 1941;28:179-213. DOI
36. Zhang J, Wang X, Xu T. Elemental selenium at nano size (Nano-Se) as a potential chemopreventive agent with reduced risk of selenium toxicity: comparison with se-methylselenocysteine in mice. *Toxicol Sci* 2008;101:22-31. DOI
37. Feng S, Liu J, Zhang X, et al. Rationalizing nitrogen-doped secondary carbon particles for practical lithium-sulfur batteries. *Nano Energy* 2022;103:107794. DOI
38. Li Q, Liu H, Yao Z, et al. Electrochemistry of selenium with sodium and lithium: kinetics and reaction mechanism. *ACS Nano* 2016;10:8788-95. DOI
39. Peng X, Wang L, Zhang X, et al. Reduced graphene oxide encapsulated selenium nanoparticles for high-power lithium-selenium battery cathode. *J Power Sources* 2015;288:214-20. DOI
40. Liu L, Hou Y, Wu X, et al. Nanoporous selenium as a cathode material for rechargeable lithium-selenium batteries. *Chem Commun* 2013;49:11515-7. DOI
41. Zhang J, Xu Y, Fan L, et al. Graphene-encapsulated selenium/polyaniline core-shell nanowires with enhanced electrochemical performance for Li-Se batteries. *Nano Energy* 2015;13:592-600. DOI
42. Wang C, Hu Q, Wei Y, Fang D, Xu W, Luo Z. Facile fabrication of selenium (Se) nanowires for enhanced lithium storage in Li-Se battery. *Ionics* 2017;23:3571-9. DOI
43. Bucur CB, Bonnick P, Jones M, Muldoon J. The evolution of selenium cathodes: from infusion melts to particle synthesis. *Sustain Energy Fuels* 2018;2:759-62. DOI
44. Xu Q, Xue H, Guo S. Status and prospects of Se_xS_y cathodes for lithium/sodium storage. *Inorg Chem Front* 2019;6:1326-40. DOI
45. Xin S, Gu L, Zhao NH, et al. Smaller sulfur molecules promise better lithium-sulfur batteries. *J Am Chem Soc* 2012;134:18510-3. DOI
46. Luo C, Zhu Y, Wen Y, Wang J, Wang C. Carbonized polyacrylonitrile-stabilized ses_x cathodes for long cycle life and high power density lithium ion batteries. *Adv Funct Mater* 2014;24:4082-9. DOI
47. Li S, Zhang W, Zeng Z, Cheng S, Xie J. Selenium or tellurium as eutectic accelerators for high-performance lithium/sodium-sulfur batteries. *Electrochem Energy Rev* 2020;3:613-42. DOI
48. Li Z, Zhang J, Wu HB, Lou XWD. An improved Li-SeS_2 Battery with high energy density and long cycle life. *Adv Energy Mater* 2017;7:1700281. DOI
49. Sun F, Cheng H, Chen J, Zheng N, Li Y, Shi J. Heteroatomic SenS8-n molecules confined in nitrogen-doped mesoporous carbons as reversible cathode materials for high-performance lithium batteries. *ACS Nano* 2016;10:8289-98. DOI
50. Khatoon R, Guo Y, Attique S, et al. Advanced configuration of n-enriched carbonized tissue paper as a free-standing interlayer for lithium-sulfur batteries at wide-range temperatures. *ACS Appl Energy Mater* 2021;4:10091-103. DOI
51. Seh ZW, Zhang Q, Li W, et al. Stable cycling of lithium sulfide cathodes through strong affinity with a bifunctional binder. *Chem Sci* 2013;4:3673. DOI
52. Wu F, Lee JT, Fan F, et al. A hierarchical particle-shell architecture for long-term cycle stability of Li_2S cathodes. *Adv Mater* 2015;27:5579-86. DOI
53. Wu F, Lee JT, Xiao Y, Yushin G. Nanostructured Li_2Se cathodes for high performance lithium-selenium batteries. *Nano Energy* 2016;27:238-46. DOI
54. Lu JG, Ye ZZ, Zeng YJ, et al. Structural, optical, and electrical properties of (Zn, Al) O films over a wide range of compositions. *J Appl Phys* 2006;100:073714. DOI
55. Schneider J, Schröder T, Hoelzel M, et al. Phase transitions to superionic Li_2Te and Li_2Se- a high-temperature neutron powder diffraction study, atom displacements, probability density functions and atom potentials. *Solid State Ion* 2018;325:90-101. DOI

56. Zuo J, Gong Y. Applications of transition-metal sulfides in the cathodes of lithium-sulfur batteries. *Tungsten* 2020;2:134-46. DOI
57. Chen H, Guo Y, Ma P, et al. Hydrothermal synthesis of Cu-doped $SnSe_2$ nanostructure for efficient lithium storage. *JEC* 2019;847:113205. DOI
58. Lei W, Xiao J, Liu H, Jia Q, Zhang H. Tungsten disulfide: synthesis and applications in electrochemical energy storage and conversion. *Tungsten* 2020;2:217-39. DOI
59. Chen H, Liu R, Wu Y, et al. Interface coupling 2D/2D $SnSe_2$/graphene heterostructure as long-cycle anode for all-climate lithium-ion battery. *Chem Eng J* 2021;407:126973. DOI
60. Xue M, Fu Z. Pulsed laser deposited Sb_2Se_3 anode for lithium-ion batteries. *J Alloys Compd* 2008;458:351-6. DOI
61. Sun C, Zhong Y, Fu W, et al. Tungsten disulfide-based nanomaterials for energy conversion and storage. *Tungsten* 2020;2:109-33. DOI
62. Xue M, Fu Z. Lithium electrochemistry of $NiSe_2$: a new kind of storage energy material. *Electrochem Commun* 2006;8:1855-62. DOI
63. Yang J, Gao H, Ma D, et al. High-performance Li-Se battery cathode based on $CoSe_2$-porous carbon composites. *Electrochim Acta* 2018;264:341-9. DOI
64. Xu GL, Ma T, Sun CJ, et al. Insight into the capacity fading mechanism of amorphous se_2S_5 confined in micro/mesoporous carbon matrix in ether-based electrolytes. *Nano Lett* 2016;16:2663-73. DOI
65. Liu L, Hou Y, Yang Y, et al. A Se/C composite as cathode material for rechargeable lithium batteries with good electrochemical performance. *RSC Adv* 2014;4:9086-91. DOI
66. Mukkabla R, Kuldeep, Killi K, Shivaprasad SM, Deepa M. Metal oxide interlayer for long-lived lithium-selenium batteries. *Chemistry* 2018;24:17327-38. DOI PubMed
67. Luo C, Wang J, Suo L, Mao J, Fan X, Wang C. In situ formed carbon bonded and encapsulated selenium composites for Li-Se and Na-Se batteries. *J Mater Chem A* 2015;3:555-61. DOI
68. Zhao Z, Xia K, Hou Y, et al. Designing flexible, smart and self-sustainable supercapacitors for portable/wearable electronics: from conductive polymers. *Chem Soc Rev* 2021;50:12702-43. DOI
69. Liu L, Wei Y, Zhang C, et al. Enhanced electrochemical performances of mesoporous carbon microsphere/selenium composites by controlling the pore structure and nitrogen doping. *Electrochim Acta* 2015;153:140-8. DOI
70. Yi Z, Yuan L, Sun D, et al. High-performance lithium-selenium batteries promoted by heteroatom-doped microporous carbon. *J Mater Chem A* 2015;3:3059-65. DOI
71. Shiraz MHA, Zhu H, Liu Y, Sun X, Liu J. Activation-free synthesis of microporous carbon from polyvinylidene fluoride as host materials for lithium-selenium batteries. *J Power Sources* 2019;438:227059. DOI
72. Yuan Y, Lu Y, Jia BE, et al. Integrated system of solar cells with hierarchical $NiCo_2O_4$ battery-supercapacitor hybrid devices for self-driving light-emitting diodes. *Nanomicro Lett* 2019;11:42. DOI PubMed PMC
73. Park GD, Kim JH, Lee J, Chan Kang Y. Carbon microspheres with well-developed micro- and mesopores as excellent selenium host materials for lithium-selenium batteries with superior performances. *J Mater Chem A* 2018;6:21410-8. DOI
74. Chen C, Zhao C, Hu Z, Liu K. Synthesis of Se/chitosan-derived hierarchical porous carbon composite as Li-Se battery cathode. *Funct Mater Lett* 2017;10:1650074. DOI
75. Qu Y, Zhang Z, Jiang S, et al. Confining selenium in nitrogen-containing hierarchical porous carbon for high-rate rechargeable lithium-selenium batteries. *J Mater Chem A* 2014;2:12255. DOI
76. Guo Y, Khatoon R, Lu J, et al. Regulating adsorption ability toward polysulfides in a porous carbon/Cu_3P hybrid for an ultrastable high-temperature lithium-sulfur battery. *Carbon Energy* 2021;3:841-55. DOI
77. Pongilat R, Nallathamby K. Size-Dependent charge storage behavior of mesoporous hollow carbon spheres for high-performance Li-Se batteries. *J Phys Chem C* 2019;123:5881-9. DOI
78. Gryglewicz G, Machnikowski J, Lorenc-grabowska E, Lota G, Frackowiak E. Effect of pore size distribution of coal-based activated carbons on double layer capacitance. *Electrochim Acta* 2005;50:1197-206. DOI
79. Babu D, Ramesha K. Constraining polyselenide formation in ether based electrolytes through confinement of Se in microporous carbon matrix for Li-Se batteries. *Electrochim Acta* 2016;219:295-304. DOI
80. Zhao C, Hu Z, Luo J. Porous carbon nanoplate/Se composite derived from potassium citrate as high-performance Li-Se battery cathode: a study on structure-function relation. *Colloids Surf A Physicochem Eng Asp* 2019;560:69-77. DOI
81. Lee JT, Kim H, Oschatz M, et al. Micro- and mesoporous carbide-derived carbon-selenium cathodes for high-performance lithium selenium batteries. *Adv Energy Mater* 2015;5:1400981. DOI
82. Li Z, Yuan L, Yi Z, Liu Y, Huang Y. Confined selenium within porous carbon nanospheres as cathode for advanced Li-Se batteries. *Nano Energy* 2014;9:229-36. DOI
83. Kalimuthu B, Nallathamby K. Optimization of structure and porosity of nitrogen containing mesoporous carbon spheres for effective selenium confinement in futuristic lithium-selenium batteries. *ACS Sustain Chem Eng* 2018;6:7064-77. DOI
84. Guo J, Wang Q, Qi C, et al. One-step microwave synthesized core-shell structured selenium@carbon spheres as cathode materials for rechargeable lithium batteries. *Chem Commun* 2016;52:5613-6. DOI
85. Zhang J, Fan L, Zhu Y, et al. Selenium/interconnected porous hollow carbon bubbles composites as the cathodes of Li-Se batteries with high performance. *Nanoscale* 2014;6:12952-7. DOI
86. Lai Y, Yang F, Zhang Z, Jiang S, Li J. Encapsulation of selenium in porous hollow carbon spheres for advanced lithium-selenium

batteries. *RSC Adv* 2014;4:39312-5. DOI

87. Li J, Zhao X, Zhang Z, Lai Y. Facile synthesis of hollow carbonized polyaniline spheres to encapsulate selenium for advanced rechargeable lithium-selenium batteries. *J Alloys Compd* 2015;619:794-9. DOI
88. Zhang Z, Yang X, Guo Z, et al. Selenium/carbon-rich core-shell composites as cathode materials for rechargeable lithium-selenium batteries. *J Power Sources* 2015;279:88-93. DOI
89. Kalimuthu B, Nallathamby K. Designed Formulation of Se-impregnated N-containing hollow core mesoporous shell carbon spheres: multifunctional potential cathode for Li-Se and Na-se batteries. *ACS Appl Mater Interfaces* 2017;9:26756-70. DOI PubMed
90. Zheng Z, Su Q, Xu H, Zhang Q, Ye H, Wang Z. A pomegranate-like porous carbon nanomaterial as selenium host for stable lithium-selenium batteries. *Mater Lett* 2019;244:134-7. DOI
91. Park S, Park J, Kang YC. Selenium-infiltrated metal-organic framework-derived porous carbon nanofibers comprising interconnected bimodal pores for Li-Se batteries with high capacity and rate performance. *J Mater Chem A* 2018;6:1028-36. DOI
92. Mukkabla R, Deshagani S, Meduri P, Deepa M, Ghosal P. Selenium/graphite platelet nanofiber composite for durable Li-Se batteries. *ACS Energy Lett* 2017;2:1288-95. DOI
93. Liu Y, Si L, Du Y, et al. Strongly bonded selenium/microporous carbon nanofibers composite as a high-performance cathode for lithium-selenium batteries. *J Phys Chem C* 2015;119:27316-21. DOI
94. Zeng L, Wei X, Wang J, et al. Flexible one-dimensional carbon-selenium composite nanofibers with superior electrochemical performance for Li-Se/Na-Se batteries. *J Power Sources* 2015;281:461-9. DOI
95. Zhang J, Zhang Z, Li Q, Qu Y, Jiang S. Selenium Encapsulated into interconnected polymer-derived porous carbon nanofiber webs as cathode materials for lithium-selenium batteries. *J Electrochem Soc* 2014;161:A2093-8. DOI
96. Feng N, Xiang K, Xiao L, et al. Se/CNTs microspheres as improved performance for cathodes in Li-Se batteries. *J Alloys Compd* 2019;786:537-43. DOI
97. Cui Y, Zhou X, Guo W, et al. Selenium nanocomposite cathode with long cycle life for rechargeable lithium-selenium batteries. *Batteries Supercaps* 2019;2:784-91. DOI
98. He J, Chen Y, Lv W, et al. Three-dimensional hierarchical graphene-CNT@Se: a highly efficient freestanding cathode for Li-Se batteries. *ACS Energy Lett* 2016;1:16-20. DOI
99. Hong YJ, Roh KC, Chan Kang Y. Mesoporous graphitic carbon microspheres with a controlled amount of amorphous carbon as an efficient Se host material for Li-Se batteries. *J Mater Chem A* 2018;6:4152-60. DOI
100. Lv H, Chen R, Wang X, et al. High-performance Li-Se batteries enabled by selenium storage in bottom-up synthesized nitrogen-doped carbon scaffolds. *ACS Appl Mater Interfaces* 2017;9:25232-8. DOI
101. Wang B, Zhang J, Xia Z, et al. Polyaniline-coated selenium/carbon composites encapsulated in graphene as efficient cathodes for Li-Se batteries. *Nano Res* 2018;11:2460-9. DOI
102. Zeng L, Chen X, Liu R, et al. Green synthesis of a Se/HPCF-rGO composite for Li-Se batteries with excellent long-term cycling performance. *J Mater Chem A* 2017;5:22997-3005. DOI
103. Han K, Liu Z, Shen J, Lin Y, Dai F, Ye H. A free-standing and ultralong-life lithium-selenium battery cathode enabled by 3D mesoporous carbon/graphene hierarchical architecture. *Adv Funct Mater* 2015;25:455-63. DOI
104. Li J, Zhang C, Wu C, Yang Q. Improved performance of Li-Se battery based on a novel dual functional CNTs@graphene/CNTs cathode construction. *Rare Metals* 2017;36:425-33. DOI
105. Ge J, Zhang Q, Liu Z, Yang H, Lu B. Solvothermal synthesis of graphene encapsulated selenium/carboxylated carbon nanotubes electrode for lithium-selenium battery. *J Alloys Compd* 2019;810:151894. DOI
106. Han K, Liu Z, Ye H, Dai F. Flexible self-standing graphene-Se@CNT composite film as a binder-free cathode for rechargeable Li-Se batteries. *J Power Sources* 2014;263:85-9. DOI
107. Fan S, Zhang Y, Li S, Lan T, Xu J. Hollow selenium encapsulated into 3D graphene hydrogels for lithium-selenium batteries with high rate performance and cycling stability. *RSC Adv* 2017;7:21281-6. DOI
108. Plaza-rivera CO, Viggiano RP, Dornbusch DA, Wu JJ, Connell JW, Lin Y. Holey graphene-enabled solvent-free preparation of ultrahigh mass loading selenium cathodes for high areal capacity lithium-selenium batteries. *Front Energy Res* 2021;9:703676. DOI
109. Palaniselvam T, Valappil MO, Illathvalappil R, Kurungot S. Nanoporous graphene by quantum dots removal from graphene and its conversion to a potential oxygen reduction electrocatalyst via nitrogen doping. *Energy Environ Sci* 2014;7:1059. DOI
110. Cai Q, Li Y, wang L, et al. Freestanding hollow double-shell Se@CN_x nanobelts as large-capacity and high-rate cathodes for Li-Se batteries. *Nano Energy* 2017;32:1-9. DOI
111. Yangdan L, Yichuan G, Yang T, Haichao T, Zhizhen Y, Jianguo L. Porous carbon derived from corncob as cathode host for Li-Se battery. *Ionics* 2022;28:2593-601. DOI
112. Yan Z, Yang Q, Wang Q, Ma J. Nitrogen doped porous carbon as excellent dual anodes for Li- and Na-ion batteries. *Chin Chem Lett* 2020;31:583-8. DOI
113. Sun S, Han F, Wu X, Fan Z. One-step synthesis of biomass derived O, N-codoped hierarchical porous carbon with high surface area for supercapacitors. *Chin Chem Lett* 2020;31:2235-8. DOI
114. Jia M, Niu Y, Mao C, et al. Porous carbon derived from sunflower as a host matrix for ultra-stable lithium-selenium battery. *J Colloid Interface Sci* 2017;490:747-53. DOI
115. Ping G, Miao L, Awati A, et al. Porous carbon globules with moss-like surfaces from semi-biomass interpenetrating polymer network for efficient charge storage. *Chin Chem Lett* 2021;32:3811-6. DOI

116. Sun K, Zhao H, Zhang S, Yao J, Xu J. Selenium/pomelo peel-derived carbon nanocomposite as advanced cathode for lithium-selenium batteries. *Ionics* 2015;21:2477-84. DOI
117. Jia M, Lu S, Chen Y, et al. Three-dimensional hierarchical porous tubular carbon as a host matrix for long-term lithium-selenium batteries. *J Power Sources* 2017;367:17-23. DOI
118. Kundu D, Krumeich F, Nesper R. Investigation of nano-fibrous selenium and its polypyrrole and graphene composite as cathode material for rechargeable Li-batteries. *J Power Sources* 2013;236:112-7. DOI
119. Zhang Z, Yang X, Wang X, Li Q, Zhang Z. TiO_2-Se composites as cathode material for rechargeable lithium-selenium batteries. *Solid State Ion* 2014;260:101-6. DOI
120. Song JP, Wu L, Dong WD, et al. MOF-derived nitrogen-doped core-shell hierarchical porous carbon confining selenium for advanced lithium-selenium batteries. *Nanoscale* 2019;11:6970-81. DOI
121. Ye W, Wang K, Yin W, et al. A novel Zr-MOF-based and polyaniline-coated UIO-67@Se@PANI composite cathode for lithium-selenium batteries. *Dalton Trans* 2019;48:10191-8. DOI
122. Tang H, Xia K, Lu J, et al. $NiTe_2$-based electrochemical capacitors with high-capacitance AC line filtering for regulating TENGs to steadily drive LEDs. *Nano Energy* 2021;84:105931. DOI
123. Tian Y, Lu J, Tang H, et al. An ultra-stable anode material for high/low-temperature workable super-fast charging sodium-ion batteries. *Chem Eng J* 2021;422:130054. DOI
124. Zhao X, Yin L, Zhang T, et al. Heteroatoms dual-doped hierarchical porous carbon-selenium composite for durable Li-Se and Na-Se batteries. *Nano Energy* 2018;49:137-46. DOI
125. Scrosati B, Hassoun J, Sun Y. Lithium-ion batteries. a look into the future. *Energy Environ Sci* 2011;4:3287. DOI
126. Du Y, Gao X, Li S, Wang L, Wang B. Recent advances in metal-organic frameworks for lithium metal anode protection. *Chin Chem Lett* 2020;31:609-16. DOI
127. Byeon A, Zhao MQ, Ren CE, et al. Two-dimensional titanium carbide mxene as a cathode material for hybrid magnesium/lithium-ion batteries. *ACS Appl Mater Interfaces* 2017;9:4296-300. DOI
128. Li D, Chen X, Xiang P, Du H, Xiao B. Chalcogenated-$Ti_3C_2X_2$ MXene (X = O, S, Se and Te) as a high-performance anode material for Li-ion batteries. *Appl Surf Sci* 2020;501:144221. DOI
129. ang C, Wang X, Zhang S. Research on metallic chalcogen-functionalized monolayer-puckered V_2CX_2 (X = S, Se, and Te) as promising Li-ion battery anode materials. *Mater Chem Front* 2021;5:4672-81. DOI
130. Eom K, Lee JT, Oschatz M, et al. A stable lithiated silicon-chalcogen battery via synergetic chemical coupling between silicon and selenium. *Nat Commun* 2017;8:13888. DOI PubMed PMC
131. Si L, Wang J, Li G, et al. High energy density lithium-selenium batteries enabled by a covalent organic framework-coated separator. *Mater Lett* 2019;246:144-8. DOI
132. Fang R, Zhou G, Pei S, Li F, Cheng HM. Localized polyselenides in a graphene-coated polymer separator for high rate and ultralong life lithium-selenium batteries. *Chem Commun* 2015;51:3667-70. DOI
133. Mukkabla R, Kuldeep, Deepa M. Poly(carbazole)-coated selenium@conical carbon nanofibers hybrid for lithium-selenium batteries with enhanced lifespan. *ACS Appl Energy Mater* 2018;1:6964-76. DOI
134. Gu X, Xin L, Li Y, et al. Highly reversible Li-Se batteries with ultra-lightweight N,S-codoped graphene blocking layer. *Nanomicro Lett* 2018;10:59. DOI PubMed PMC
135. Yang Z, Zhu K, Dong Z, Jia D, Jiao L. Stabilization of Li-Se batteries by wearing pan protective clothing. *ACS Appl Mater Interfaces* 2019;11:40069-77. DOI PubMed
136. Zhang Z, Zhang Z, Zhang K, Yang X, Li Q. Improvement of electrochemical performance of rechargeable lithium-selenium batteries by inserting a free-standing carbon interlayer. *RSC Adv* 2014;4:15489-92. DOI
137. Zhang Z, Cao H, Yang M, et al. High performance room temperature all-solid-state Na-Se S battery with Na_3SbS_4-coated cathode via aqueous solution. *J Energy Chem* 2020;48:250-8. DOI
138. Li X, Liang J, Kim JT, et al. Highly stable halide-electrolyte-based all-solid-state li-Se batteries. *Adv Mater* 2022;34:e2200856. DOI
139. Huang D, Li S, Luo Y, et al. Graphene oxide-protected three dimensional Se as a binder-free cathode for Li-Se battery. *Electrochim Acta* 2016;190:258-63. DOI
140. Xia Y, Lu C, Fang R, et al. Freestanding layer-structure selenium cathodes with ultrahigh Se loading for high areal capacity Li-Se batteries. *Electrochem Commun* 2019;99:16-21. DOI
141. Zhou X, Gao P, Sun S, et al. Amorphous, crystalline and crystalline/amorphous selenium nanowires and their different (de)lithiation mechanisms. *Chem Mater* 2015;27:6730-6. DOI
142. Xue M, Fu Z. Electrochemical reactivity mechanism of $CuInSe_2$ with lithium. *Thin Solid Films* 2008;516:8386-92. DOI
143. Jiang S, Zhang Z, Lai Y, et al. Selenium encapsulated into 3D interconnected hierarchical porous carbon aerogels for lithium-selenium batteries with high rate performance and cycling stability. *J Power Sources* 2014;267:394-404. DOI
144. Lai Y, Gan Y, Zhang Z, Chen W, Li J. Metal-organic frameworks-derived mesoporous carbon for high performance lithium-selenium battery. *Electrochim Acta* 2014;146:134-41. DOI
145. Qu Y, Zhang Z, Lai Y, Liu Y, Li J. A bimodal porous carbon with high surface area supported selenium cathode for advanced Li-Se batteries. *Solid State Ion* 2015;274:71-6. DOI
146. Zhou J, Yang J, Xu Z, Zhang T, Chen Z, Wang J. A high performance lithium-selenium battery using a microporous carbon confined selenium cathode and a compatible electrolyte. *J Mater Chem A* 2017;5:9350-7. DOI

147. Lian J, Wu Y, Guo Y, et al. Design of hierarchical and mesoporous FeF_3/rGO hybrids as cathodes for superior lithium-ion batteries. *Chin Chem Lett* 2022;33:3931-5. DOI
148. Tang H, Tian Y, Wu Z, et al. AC line filter electrochemical capacitors: materials, morphology, and configuration. *Energy Environ Mater* 2022;5:1060-83. DOI
149. Chen D, Zhao Z, Chen G, et al. Metal selenides for energy storage and conversion: a comprehensive review. *Coord Chem Rev* 2023;479:214984. DOI
150. Khatoon R, Attique S, Liu R, et al. Carbonized waste milk powders as cathodes for stable lithium-sulfur batteries with ultra-large capacity and high initial coulombic efficiency. *Green Energy Environment* 2022;7:1071-83. DOI